

Solar: a least-angle regression for accurate and stable variable selection in high-dimensional data

Ning Xu, Jian Hong and Timothy C.G. Fisher

*School of Economics, University of Sydney
NSW 2006 Australia*

e-mail: n.xu@sydney.edu.au; jian.hong@sydney.edu.au; tim.fisher@sydney.edu.au

Abstract: We propose a new least-angle regression algorithm for variable selection in high-dimensional data, called *subsample-ordered least-angle regression (solar)*. Solar relies on the average L_0 solution path computed across subsamples and largely alleviates several known high-dimensional issues with least-angle regression. Using examples based on directed acyclic graphs, we illustrate the advantages of solar in comparison to least-angle regression, forward regression and variable screening. Simulations demonstrate that, with a similar computation load, solar yields substantial improvements over two lasso solvers (least-angle regression for lasso and coordinate-descent) in terms of the sparsity (37-64% reduction in the average number of selected variables), stability and accuracy of variable selection. Simulations also demonstrate that solar enhances the robustness of variable selection to different settings of the irrepresentable condition and to variations in the dependence structures assumed in regression analysis. We provide a Python package `solarpy` for the algorithm (<https://github.com/isaac2math/solar>).

Keywords and phrases: variable selection, forward regression, least-angle regression, lasso regression, coordinate descent, K -fold cross-validation.

1. Introduction

Consider variable selection in lasso regression,

$$\min_{\beta} \frac{1}{2} \|Y - X\beta\|_2^2 + \lambda \|\beta\|_1 \quad (1.1)$$

where $Y \in \mathbb{R}^{n \times 1}$ is the response variable, $X \in \mathbb{R}^{n \times p}$ is a matrix of covariates, $\beta \in \mathbb{R}^{p \times 1}$ is a vector of regression coefficients, $\|\cdot\|_v$ is the L_v norm, and λ is the tuning or penalty parameter. The variance of each column in X is 1 (i.e., standardized). In this paper we focus on high-dimensional data, i.e., the case of $p \geq n$, where variable selection is always required. In this context, we define **informative variables** and **redundant variables** as follows.

Definition 1.1 (informative and redundant variables). Conditional on all other variables (in X or not), define \mathbf{x}_i (the i^{th} column of X) to be an **informative variable** if it has a non-zero correlation to Y in the population; otherwise define \mathbf{x}_i to be a **redundant variable**.

The *least absolute shrinkage and selection operator (lasso)* is among the most widely used high-dimensional variable-selection methods. As one of the most efficient numerical optimizers for lasso, least-angle regression has been widely applied across many fields, including

text mining and natural language processing in machine learning, DNA analysis in biostatistics, signal-processing and compressed-sensing in engineering. Using least-angle regression as the blueprint, various lasso-type estimators have been constructed for a range of learning tasks and, in particular, modifications to least-angle regression and lasso have been proposed to improve variable-selection accuracy and stability. Unfortunately, the improvements have often come at the cost of a higher computation load. In a world of ever-expanding data dimensions, it is increasingly important to improve the variable-selection performance of lasso and least-angle regression while restraining the computation load.

Furthermore, increases in data dimensions are typically associated with more severe multicollinearity and more complicated dependence structures, adding to the challenges of variable selection. These challenges compel variable-selection algorithms to utilize as much relevant finite-sample information as possible to enhance the accuracy, stability and robustness of variable-selection methods in high dimensional spaces.

In this paper, we propose a new least-angle regression algorithm for high-dimensional data, called *subsample-ordered least-angle regression (solar)*. Solar relies on the average L_0 solution path computed across subsamples and significantly mitigates several known high-dimensional issues with least-angle regression. Using directed acyclic graphs and examples, we compare solar with least-angle regression, forward regression and variable screening. We illustrate in simulations that, with a similar computation load, solar yields substantial improvements over two lasso solvers (least-angle regression for lasso and coordinate-descent) in terms of the sparsity, stability and accuracy of variable selection. We also illustrate numerically that solar enhances the robustness of variable selection to different settings of the irrerepresentable condition and to variations in the dependence structures assumed in regression analysis.

1.1. Variable-selection techniques for least-angle regression and lasso

Tibshirani (1996) first introduced lasso as a shrinkage method for the purposes of high-dimensional variable selection. Many elegant theoretical properties (such as variable-selection consistency, L_2 consistency and error bounds) have subsequently been established (Knight and Fu, 2000; Zhao and Yu, 2006; Meinshausen and Yu, 2009; Bickel et al., 2009; Candès et al., 2009). Lasso has been generalized to different scenarios, producing fused lasso (Tibshirani et al., 2005), elastic net (Zou and Hastie, 2005), adaptive lasso (Zou, 2006), graphical lasso (Friedman et al., 2008) and group lasso (Friedman et al., 2010). Owing to the high computational load of the lasso-type estimators, alternative numerical optimizers have been developed, including least-angle regression (Efron et al., 2004) and coordinate descent (Wu et al., 2008).

As a modification of the forward regression algorithm—summarized in Algorithm 1—least-angle regression is well-known for ultra-fast computation and adaptability to lasso-type estimators. To avoid confusion, we specify the meaning of forward regression and least-angle regression as follows.

Definition 1.2 (Forward regression, least-angle regression and its lasso modification).

- We refer to the generic forward regression algorithm (Algorithm 1) as **forward regression**.

- We refer to the least-angle regression without the lasso modification (Algorithm 3.2 in Friedman et al. (2001)) as **lars**.
- We refer to the least-angle regression with the lasso modification (Algorithm 3.2a in Friedman et al. (2001)) as **lars-lasso**, which drops \mathbf{x}_i if β_i hits 0 on the solution path.
- If \mathbf{x}_j is chosen by forward regression at stage l (i.e., $i^* = j$ in the l^{th} iteration of the for-loop in Algorithm 1), we say that \mathbf{x}_j is **included** at stage l . If \mathbf{x}_j is returned with a non-zero regression coefficient at the end of the lars-lasso or forward regression algorithm, we say \mathbf{x}_j is **selected**.

Algorithm 1: Forward regression (Zhang, 2009)

```

input :  $(Y, X)$ ,  $\epsilon$ .
1 standardize all  $\{\mathbf{x}_i\}$  in  $X$ ;
2 let  $F = \emptyset$  and  $\beta = \mathbf{0}$ ;
3 for  $l := 1$  to  $\min\{n, p\}$ ,  $stepsize = 1$  do
4   | let  $i^* = \arg \max_i |\mathbf{x}_i^T (X\beta - Y)|$ ;
5   | if  $\epsilon$  is preset and  $|\mathbf{x}_{i^*}^T (X\beta - Y)| < \epsilon$  then
6   |   | Break the for-loop
7   | end
8   | let  $F = F \cup \{i^*\}$ ;
9   | let  $\beta$  be the OLS regression coefficient estimate on support  $F$ ;
10 end
11 if  $\epsilon$  is not preset then
12   | choose the optimal value of  $\epsilon$  via CV or BIC;
13   | based on the optimal value of  $\epsilon$ , redo line 3 to 10;
14 end
15 return  $\beta$  and  $F$ 

```

Compared to forward regression, equiangular search in least-angle regression has a higher tolerance for multicollinearity in the X variables. Friedman et al. (2010) shows in some cases that lars-lasso has a lower computation load than coordinate descent: lars-lasso finishes tuning-parameter optimization in one training round; coordinate descent requires repeated training rounds for each value of λ in the grid search.¹ While lars-lasso is computationally efficient, Weisberg (2004) argues it may still be sensitive to sampling randomness, multicollinearity, noise and outliers in high-dimensional spaces due to the iterative refitting of the residual.

Optimization of the tuning parameter in lasso is often combined with cross validation (CV) (Stone, 1974, 1977), which itself has several well-documented problems. Xu et al. (2012) argues that the computation load of CV may be substantial when tuning parameters in complex models. In large-scale simulations, Cawley and Talbot (2010) show that a high

¹Friedman et al. (2010) comment that the time difference between R packages ‘glmnet’ and ‘lars’ (for lars-lasso) in their paper is due to the fact that ‘glmnet’ is coded in Fortran and ‘lars’ is coded in R, which is considered to be less efficient than Fortran. By contrast, in the Google open-source package Sci-kit Learn, both coordinate descent and lars-lasso are coded in Python and lars-lasso is demonstrated to be much faster than coordinate descent in a number of applications.

CV variance complicates variable selection, leading to problems with selection stability. [Nan and Yang \(2014\)](#); [Lim and Yu \(2016\)](#) point out that the ‘stability issue of model selection’ is more severe in high-dimensional spaces. [Lim and Yu \(2016\)](#) shows that CV-based lasso may lead to models that are unstable in high dimensions and consequently ill-suited for interpretation and generalization.

Different methods have been proposed to improve the variable-selection accuracy and stability of CV-based lasso. Subsampling is a common approach to purge redundant variables incorrectly selected by lasso. For example, [Bach \(2008\)](#) proposes training one CV-based lasso on each bootstrap set and combining results across bootstrap sets. In a similar vein, [Meinshausen and Bühlmann \(2010\)](#) propose using repeated randomization in place of bootstrapping. Given the fact that CV-based lasso merges the computation loads of lasso and CV, repeating CV-based lasso many times magnifies the computation load, particularly in high-dimensional data (e.g., in text mining or natural language processing p could be in the millions).

Another approach to improve accuracy is to conduct post-lasso selection on variables chosen by coordinate descent optimization. [Ghaoui et al. \(2010\)](#) and [Tibshirani et al. \(2012\)](#) propose two post-lasso selection rules called the ‘safe rule’ and the ‘strong rule’, further developed by [Wang et al. \(2014\)](#) and [Wang et al. \(2016\)](#). Claiming both rules may incorrectly purge informative variables, [Zeng et al. \(2017\)](#) proposes an alternative ‘hybrid safe-strong rule’ as the solution.

An alternative approach to improving accuracy uses post-estimation statistical tests of the variables selected by lars-lasso, e.g., the covariance test ([Lockhart et al., 2014](#)). Yet the sensitivity of lars-lasso to sampling randomness, multicollinearity, noise and outliers noted by [Weisberg \(2004\)](#) means that post-estimation tests may be unreliable. Thus, one way to make post-estimation tests more reliable is to resolve the lars-lasso sensitivity issue.

Besides lasso, some researchers have applied the variable screening method (also referred to as marginal correlation ranking) to variable selection in regression analysis (e.g., [Fan and Lv \(2008\)](#); [Hall and Miller \(2009\)](#); [Hall et al. \(2009\)](#)). The method ranks variables decreasingly based on the absolute values of their marginal correlations to Y and selects the top w variables (where w is selected by CV, bootstrap or BIC). Various correlation coefficients have been used to improve the accuracy of the marginal correlation ranking method (e.g., [Li et al. \(2012b\)](#); [Cho and Fryzlewicz \(2012\)](#); [Li et al. \(2012a\)](#); [Shao and Zhang \(2014\)](#)).

1.2. Motivating examples

To illustrate the accuracy and stability issues in the context of variable selection with high-dimensional data, we consider two well-known examples from the literature.

Throughout the paper we use directed acyclic graphs to describe data generating processes. Figure 1 displays the directed acyclic graph for an example of the dependence structure typically assumed in the theoretical and numerical regression analysis, referred to as the *standard dependence structure* in this paper.

In a directed acyclic graph, arrows represent causation. For example, the arrow from \mathbf{x}_1 to Y in Figure 1 means that \mathbf{x}_1 *causes* Y . Figure 1 represents the case where \mathbf{x}_1 and \mathbf{x}_2 cause Y , indicating that $\{\mathbf{x}_1, \mathbf{x}_2\}$ are informative, $\{\mathbf{x}_3, \mathbf{x}_4, \dots\}$ are not related to Y , indicating that they are redundant, while e is a standard Gaussian noise term. We also use the terminology

that $\{\mathbf{x}_1, \mathbf{x}_2\}$ are the ‘parents’ of Y , Y is the ‘child’ of $\{\mathbf{x}_1, \mathbf{x}_2\}$ and \mathbf{x}_1 is a ‘spouse’ of \mathbf{x}_2 .² Thus, variable selection with the standard dependence structure can be thought of as ‘parent selection’, where Y is assumed to be an ‘only child’ and redundant variables are ‘not related’ to Y . Note that the informative variables $\{\mathbf{x}_1, \mathbf{x}_2\}$ are marginally and conditionally *correlated* with Y and the redundant variables $\{\mathbf{x}_3, \mathbf{x}_4, \dots\}$ are marginally and conditionally *uncorrelated* with Y . Discussion of the case where some of the informative variables are latent is available in supplementary file A.

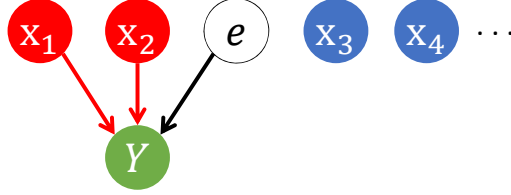


Fig 1: Standard dependence structure in regression analysis (arrows denote causation).

We use directed acyclic graphs to illustrate two examples from the literature. Example 1 shows that lasso may have a variable-selection stability problem when the standard dependence structure is assumed. Example 2 shows that lasso may have a variable-selection accuracy issue when the standard dependence structure is violated.

Example 1. (Lim and Yu, 2016) consider the lars-lasso algorithm. To reduce the computation load, lars-lasso uses the L_1 -norm fraction $t \in [0, 1]$ as a tuning parameter to control shrinkage. In each CV training-validation split, for all β on the solution path, t is defined as the ratio of $\|\beta\|_1$ to the L_1 norm of the non-shrunked solution on the solution path (referred to as $\|\beta_{\max}\|_1$), i.e.

$$t = \frac{\|\beta\|_1}{\|\beta_{\max}\|_1}, \quad (1.2)$$

where $t = 0$ corresponds to shrinking all β_i to 0 and $t = 1$ corresponds to no shrinkage.

Lim and Yu (2016) show that the solution path of lars-lasso is unstable in high dimensions. When $p > n$, the non-shrunked least-angle regression solution (β_{\max}) is the traditional forward regression solution with n selected variables. With $p > n$, the non-shrunked least-angle regression solution uses up all n degrees of freedom (a saturated fit), implying, due to the resampling randomness in CV, that $\|\beta_{\max}\|_1$ may vary substantially across validation sets. As a result, the same value of t may correspond to different amounts of shrinkage (or λ) on the solution paths of different CV training-validation splits, limiting the usefulness of t as a shrinkage parameter and adversely impacting the selection accuracy and stability of CV-based lars-lasso.

Figure 2 shows the histogram for $\|\beta_{\max}\|_1$ from 10,000 bootstrap lasso estimates from a Gaussian simulation where the variance of each variable is 1, pairwise correlations are 0.5, $n = 100$ and $p = 150$ (Lim and Yu, 2016, Section 3.1.1.). The spread of the distribution—the

²See (Koller and Friedman, 2009, Section 2.2) for further detail on the terminology.

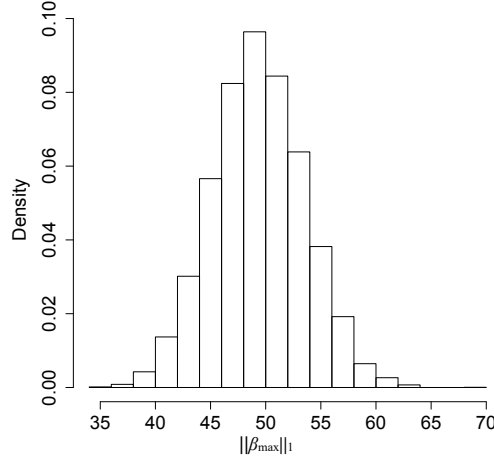


Fig 2: (Lim and Yu, 2016) Histogram of $\|\beta_{\max}\|_1$ from lasso estimates on simulated data.

difference between the upper and lower decile is more than 20—illustrates the CV-based lars-lasso stability problem. The larger $(p-n)$, the more severe the stability problem. Simulation 2 below investigates the accuracy of variable selection for various cases when $p > n$ given a standard dependence structure.

Example 2. (Zhao and Yu, 2006) Consider the following dependence structure

$$\begin{cases} \mathbf{x}_3 = \omega \mathbf{x}_1 + \omega \mathbf{x}_2 + \sqrt{1 - 2\omega^2} \cdot u \\ Y = \beta_1 \mathbf{x}_1 + \beta_2 \mathbf{x}_2 + \delta e \end{cases} \quad (1.3)$$

where the \mathbf{x}_i are standardized; e and u are independent Gaussian noise terms; δ , ω , β_1 and β_2 are scalars. As shown in Figure 3, the dependence structure is more complicated than the standard dependence structure: Y now has two parents and a ‘sibling’. Since only \mathbf{x}_1 and \mathbf{x}_2 are informative variables in (1.3), an accurate variable-selection algorithm should select only \mathbf{x}_1 and \mathbf{x}_2 . The fundamental condition for variable-selection accuracy and consistency of lasso and forward regression (Zhao and Yu, 2006; Zhang, 2009) (see Definition 2.1), the irrepresentable condition (IRC), may or may not be satisfied depending on the values of ω , β_1 and β_2 . Loosely speaking, IRC requires that the informative variables cannot explain ‘too much’ of the variation in any redundant variable. Absent IRC, the variable-selection algorithm may have difficulty identifying the informative variables.

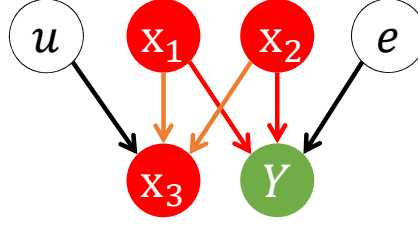


Fig 3: (Zhao and Yu, 2006) Example 2 dependence structure with latent u and e .

In simulations, Zhao and Yu (2006) set $\delta = 1$, $\omega = \frac{2}{3}$, $\beta_2 = 3$ and $n = 1,000$ with (a) $\beta_1 = 2$, implying strong IRC fails, and (b) $\beta_1 = -2$, implying strong IRC holds. The solution paths (solved by lars-lasso) from the lasso regression of Y on x_1 , x_2 and x_3 are shown in Figure 4. In (a), lars-lasso prefers the x_3 sibling of Y over the true parents x_1 and x_2 , wrongly selecting x_3 as an informative variable. Lars-lasso does not make the same mistake in (b) when strong IRC is satisfied.

The challenge in Example 2 is the strong multicollinearity resulting from the non-standard dependence structure, a problem that may be pervasive in empirical research. The standard structure in Figure 1 assumes that redundant variables are neither parent(s) nor children of the informative variables, implying violation of IRC is unlikely. However, in Example 2 the redundant variables and informative variables are causally related, resulting in strong multicollinearity. The strong multicollinearity may violate IRC and induce errors into variable selection. Clearly, the robustness of variable selection to strong multicollinearity and non-standard dependence structures is an important empirical issue. In Simulation 3 below, we use a dependence structure similar to Example 2 to investigate the accuracy of variable selection under different settings of the IRC in high dimensions.

1.3. Main results

In this paper, we introduce a stabilized least-angle regression algorithm called *subsample-ordered least-angle regression (solar)*. Unlike traditional forward regression or lars-lasso, solar is based on the average L_0 solution path from least-angle regression on multiple subsamples. As such, solar substantially mitigates several issues faced by least-angle regression and forward regression in high-dimensional spaces. Solar has a very similar computation load to lars-lasso. Further, solar is more robust to non-standard dependence structures in regression analysis and potentially generalizable to variable selection with a variety of lasso-type and forward regression estimators. We provide the necessary pseudo-code and Python package for solar.

We illustrate the following attributes of solar using simulations: (1) when p/n approaches 0 rapidly, with the same computation load as lars-lasso, solar is more responsive to decreases in p/n , yielding significant improvements in variable-selection performance over K -fold, cross-validated least-angle regression for lasso (CV-lars-lasso, for short) and cross-validated, cyclic pathwise coordinate descent with warm start (CV-cd, for short); (2) when n and p both increase rapidly in high-dimensional space, solar significantly outperforms CV-lars-lasso and

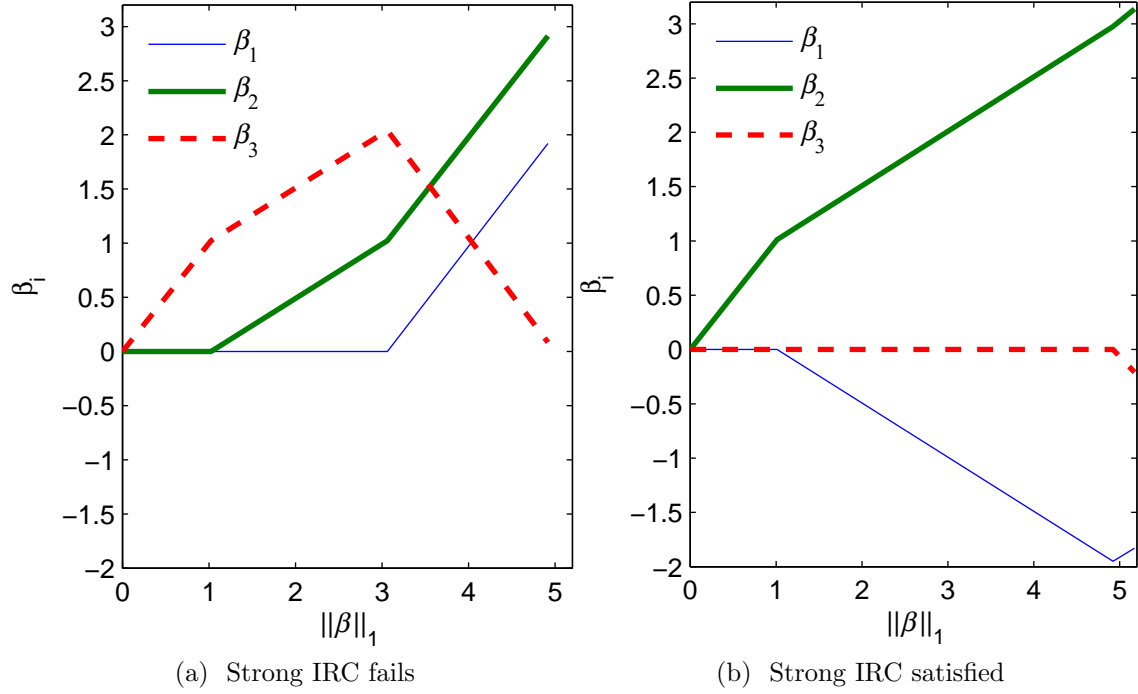


Fig 4: (Zhao and Yu, 2006) Example 2: variable selection with lars-lasso.

CV-cd in terms of convergence tendency, sparsity (a 37-64% reduction in the average number of selected variables), stability and accuracy of variable selection in high-dimensional spaces; (3) solar is robust to non-standard dependence structures in regression analysis, implying better variable-selection accuracy compared with CV-lars-lasso under different settings of the IRC. Our simulation results suggest that solar may lead to substantial improvements for forward regression, lasso-type estimators and the lasso-based ensemble algorithms (e.g., Bach (2008) and Meinshausen and Bühlmann (2010)) without increasing the computation load.

The paper is organized as follows. In section 2, we introduce solar and compare it with other variable-selection methods. In section 3, we illustrate the stepwise computation of solar and discuss its computation load. In section 4, we demonstrate the improvements of solar over lars-lasso using a comprehensive set of simulations, in which CV-lars-lasso and CV-cd are the competitors.

2. Solar: subsample ordered least-angle regression

In this section, we introduce solar and illustrate with a few examples its potential advantages over commonly used variable-selection methods. To keep the exposition precise, we first set up our notation.

Definition 2.1 (Notation).

1. Given a generic vector $w \in \mathbb{R}^{d \times 1}$, define $\text{supp}(w) = \{j \mid w_j \neq 0\}$. For any variable-selection algorithm, define the *active set* $F \subset \{1, \dots, d\}$ as the set of indices for the

selected variables and $|F|$ as the cardinality of F . Given a sample $X \in \mathbb{R}^{n \times p}$ and $Y \in \mathbb{R}^{n \times 1}$, define

$$\begin{aligned} \beta(F, Y) &= \arg \min_{\beta} \frac{1}{2} \|Y - X\beta\|_2^2 \\ \text{s.t. } \text{supp}(\beta) &\subset F. \end{aligned} \quad (2.1)$$

2. Let $\{(Y^k, X^k) \mid k = 1, \dots, K\}$ be subsamples of equal size, randomly sampled without replacement from (X, Y) . Let n_{sub} be the size of each subsample and denote $\tilde{p} = \min\{n_{\text{sub}}, p\}$. Given $F \subset \{1, \dots, d\}$, define X_F to be the $n \times |F|$ matrix with columns $\{\mathbf{x}_j \mid j \in F\}$. Based on [Tropp \(2004\)](#) and [Wainwright \(2009\)](#), define

$$\begin{aligned} \mu(F) &= \max \left\{ \left\| \left((X_F)^T X_F \right)^{-1} (X_F)^T \mathbf{x}_j \right\|_1 \mid \forall j \notin F \right\} \\ \rho(F) &= \min \left\{ \frac{1}{2} \|Xb\|_2^2 / \|b\|_2^2 \mid \text{supp}(b) \subset F \right\} \end{aligned}$$

with values $\mu_k(F)$ and $\rho_k(F)$ on each subsample.

3. Given a constant $1 \geq \eta > 0$, the **strong irrepresentable condition** is satisfied if $\mu_k(F) \leq 1 - \eta$ and the **weak irrepresentable condition** is satisfied if $\mu_k(F) < 1$.
4. At stage l of forward regression, denote the coefficients to be $\beta(l)$, $F(l) = \text{supp}(\beta(l))$, the regression residual $e(l) = Y - X\beta(l)$ and $\epsilon(l) = \max \left\{ \left| (\mathbf{x}_j)^T e(l) \right| \mid \forall j \notin F(l) \right\}$.

Several remarks apply to the definitions. The irrepresentable condition (first defined in [Zhao and Yu \(2006\)](#)) is a sufficient and (almost) necessary condition for variable-selection consistency of lasso and forward regression.³ We discuss the IRC in more detail in sections 4.3. Lastly, $\epsilon(l)$ measures the largest covariation between \mathbf{x}_j and the regression residual e at stage l . To keep the exposition in the paper concise, we rule out perfect collinearity among the informative variables and assume that Y is uniquely represented by a regression on the informative variables in the population.

To avoid confusion, we also need to define the solution path for forward regression (including lars). In the literature, the definition of the solution path depends on the research question. The solution path for forward regression is the trajectory of the β_i at each stage. For L_1 shrinkage (lars-lasso), the solution path (also referred to as the L_1 arc) can also be defined as the trajectory of the β_i at each value of $\|\beta\|_1$ (as in Figure 4) or each value of the L_1 ratio t (as in the R package ‘lars’ in [Hastie and Efron \(2013\)](#)). Since we focus on variable selection accuracy, the only relevant feature of β_i is whether $\beta_i = 0$ (or $\|\beta_i\|_0 = 0$) at each stage. Thus, we define the solution path as follows.

Definition 2.2 (L_0 solution path). Define the L_0 **solution path** of forward regression on (Y^k, X^k) to be the order that forward regression includes variables across all stages. For example, in Figure 4a, lars-lasso includes \mathbf{x}_3 at stage 1, \mathbf{x}_2 at stage 2 and \mathbf{x}_1 at stage

³The IRC takes different forms in the literature. Definition 2.1 follows [Tropp \(2004\)](#), [Zhang \(2009\)](#) and [Wainwright \(2009\)](#). While the [Zhao and Yu \(2006\)](#) definition takes a different form to Definition 2.1 the two are equivalent. [Zhao and Yu \(2006\)](#) shows that IRC is closely related to $\tilde{\beta}(z)$, the coefficients from a regression of a redundant variable z on all the informative variables. When the signs of the true β are unknown, weak IRC requires $\|\tilde{\beta}(z)\|_1 < 1$ and strong IRC requires $\|\tilde{\beta}(z)\|_1 < 1 - \eta$, for any redundant variable z .

3. As a result, the L_0 solution path of lars-lasso can be represented as an ordered set $\{\{\mathbf{x}_3\}, \{\mathbf{x}_3, \mathbf{x}_2\}, \{\mathbf{x}_3, \mathbf{x}_2, \mathbf{x}_1\}\}$.

The L_0 solution path plays a vital role in this paper. Given a fixed dimension of X and constant population variance of Y and assuming IRC is satisfied, Zhang (2009, Theorem 2) implies the earlier forward regression stops, the more likely the variables selected are informative. As a result, the L_0 solution path may be used to identify informative variables.

2.1. Average L_0 solution path estimation

The L_0 solution path is the foundation of forward regression. To stabilize least-angle regression in high-dimensional spaces, we first reduce the sensitivity of its solution path in cases where $p > n$. The *average L_0 solution path estimation* algorithm (summarized in Algorithm 2 and illustrated in Figure 5) accomplishes this task by estimating the *average stage \mathbf{x}_i enters the solution path* of lars.

Algorithm 2: average L_0 solution path estimation

input : (Y, X) .

- 1 generate K subsamples $\{(Y^k, X^k)\}_{k=1}^K$;
- 2 set $\tilde{p} = \min\{n_{\text{sub}}, p\}$;
- 3 **for** $k := 1$ to K , *stepsize* = 1 **do**
- 4 run an unrestricted lars (Algorithm 3.2 in Friedman et al. (2001)) on (Y^k, X^k) and record the order of variable inclusion at each stage^a;
- 5 define $\hat{q}^k = \mathbf{0} \in \mathbb{R}^p$;
- 6 for all i and l , if \mathbf{x}_i is included at stage l , set $\hat{q}_i^k = (\tilde{p} + 1 - l)/\tilde{p}$, where \hat{q}_i^k is the i^{th} entry of \hat{q}^k ;
- 7 **end**
- 8 $\hat{q} := \frac{1}{K} \sum_{k=1}^K \hat{q}^k$;
- 9 **return** \hat{q}

^aAlgorithm 3.2 in Friedman et al. (2001) omits the lasso modification that drops \mathbf{x}_i when β_i hits 0. Lars-lasso is Algorithm 3.2a in Friedman et al. (2001). To incorporate lars-lasso into Algorithm 2, simply add the requirement at the end of line 6 that if \mathbf{x}_i is included at some stage of lars and its regression coefficient β_i hits 0 at a later stage, set $\hat{q}_i^k = 0$. This additional requirement may be helpful in high-dimensional data with very small n .

The first step in Algorithm 2 is, without loss of generality, to generate subsamples without replacement. The next step (lines 4-6) is to compute \hat{q}^k , which summarizes the order that lars includes each \mathbf{x}_i across all stages (as in the Figure 5 example). As shown in line 6 of Algorithm 2 and Figure 5, for lars on (Y^k, X^k) , variables included at earlier stages have larger corresponding \hat{q}_i^k values: the first variable included is assigned 1, the last is assigned $1/\tilde{p}$ and the dropped variables are assigned 0 (which occurs only when $p > n$). Thus, by (decreasingly) ranking the \mathbf{x}_i according to their corresponding \hat{q}_i^k values, we obtain the L_0 solution path of lars. The Zhang (2009, Theorem 2) result implies that the variables with the largest \hat{q}_i^k values, on average, are more likely to be informative variables.

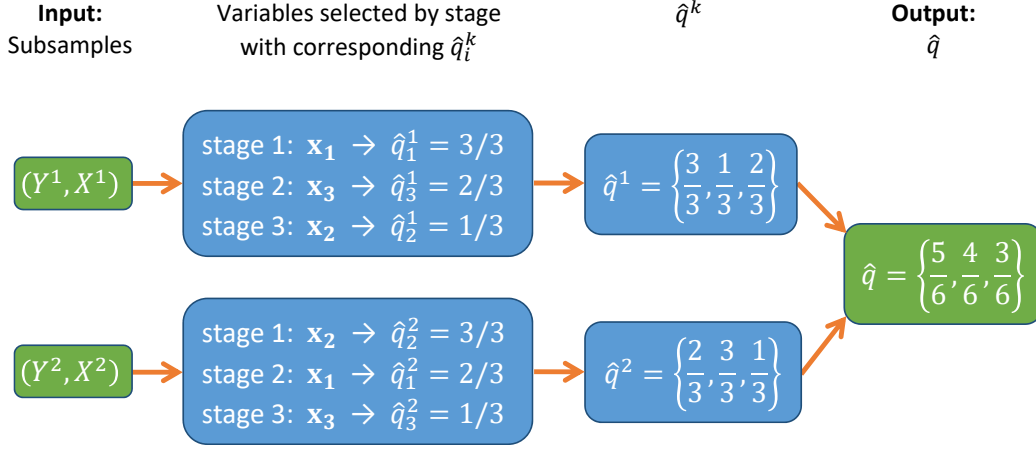


Fig 5: Computation of \hat{q} on 2 subsamples, where $\{\mathbf{x}_1, \mathbf{x}_2\}$ are informative and \mathbf{x}_3 is redundant.

The third step in Algorithm 2 (lines 3-8) is to reduce the impact of sensitivity in the \hat{q}_i^k values. The \hat{q}_i^k may be sensitive because they are computed using lars, which is sensitive in high-dimensional spaces to multicollinearity, sampling randomness and noise. A consequence of the sensitivity is that a redundant variable may be included at an early stage in some subsample (Y^k, X^k) . Consider the example in Figure 5, where \mathbf{x}_1 and \mathbf{x}_2 are informative and \mathbf{x}_3 is redundant. In subsample (Y^1, X^1) at stage 2, the redundant variable \mathbf{x}_3 is included, implying \hat{q}_3^1 (the \hat{q}_i^k value for \mathbf{x}_3 in (Y^1, X^1)) is larger than \hat{q}_2^1 (the \hat{q}_i^k value for the informative variable \mathbf{x}_2 in (Y^1, X^1)). Thus, to reduce the impact of sensitivity in the \hat{q}_i^k , we compute $\hat{q} := \frac{1}{K} \sum_{k=1}^K \hat{q}^k$ and rank the \mathbf{x}_i (decreasingly) based on the corresponding value of \hat{q}_i (the i^{th} entry of \hat{q}), to get the average L_0 solution path. The formal definition of the average L_0 solution path is as follows.

Definition 2.3 (average L_0 solution path). Define the **average L_0 solution path** of forward regression on $\{(Y^k, X^k)\}_{k=1}^K$ to be the decreasing order of variables based on their corresponding \hat{q}_i values. For example, in Figure 5, the \hat{q}_i values for \mathbf{x}_1 , \mathbf{x}_2 and \mathbf{x}_3 are, respectively, $\hat{q}_1 = 5/6$, $\hat{q}_2 = 4/6$ and $\hat{q}_3 = 3/6$. As a result, the average L_0 solution path can be represented as an ordered set $\{\{\mathbf{x}_1\}, \{\mathbf{x}_1, \mathbf{x}_2\}, \{\mathbf{x}_1, \mathbf{x}_2, \mathbf{x}_3\}\}$.

The idea behind averaging \hat{q}^k is simple and intuitive. While on some subsample(s) a redundant variable may be included at an early stage, the informative variables, on average, should be included in forward regression before the redundant variables, implying that, on average, the corresponding \hat{q}_i^k values for the informative variables should be larger than the \hat{q}_i^k values for the redundant variables. Equivalently, the corresponding \hat{q}_i values for the informative variables should be larger than \hat{q}_i values for the redundant variables. Hence, to select informative variables quickly and accurately, it is natural to focus on variables with large \hat{q}_i .

Discussion: advantages of the average L_0 solution path in non-standard dependence structures

Compared with other variable selection methods, the average L_0 solution path is more likely to be reliable in the presence of non-standard dependence structures, i.e., those that do not match the Figure 1 structure. We illustrate the point with the following two examples.

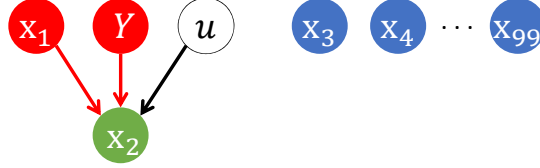


Fig 6: Collider structure of \mathbf{x}_2 with latent u .

In Figure 6, we consider the case where variable selection is more than ‘parent selection’. Specifically, Y has two informative variables: a spouse (\mathbf{x}_1) and a child (\mathbf{x}_2). Figure 6 depicts a common scenario in empirical regression: *informative variables* may be *marginally uncorrelated to Y* in the DGP. In data with such dependence structures, Example 3 demonstrates that forward regression (including solar and lars-lasso) is likely to be more reliable than post-lasso selection rules and variable screening.

Example 3. In the Figure 6 dependence structure there are 100 variables and \mathbf{x}_2 is (causally) generated by its parents $\{\mathbf{x}_1, Y\}$ as follows,

$$\mathbf{x}_2 = \alpha_1 \mathbf{x}_1 + \alpha_2 Y + u, \quad (2.2)$$

where \mathbf{x}_1 is marginally uncorrelated with Y , \mathbf{x}_1 and Y are marginally and conditionally uncorrelated with any redundant variable, $\{\alpha_1, \alpha_2\}$ are population regression coefficients and u is a Gaussian noise term. If Y is chosen to be the response variable, we have the population regression equation

$$Y = -\frac{\alpha_1}{\alpha_2} \mathbf{x}_1 + \frac{1}{\alpha_2} \mathbf{x}_2 - \frac{1}{\alpha_2} u. \quad (2.3)$$

Note that \mathbf{x}_1 and \mathbf{x}_2 are both informative variables for Y based on Definition 1.1. However, since \mathbf{x}_1 is marginally uncorrelated with Y in the population, post-lasso variable selection rules may be prone to purging \mathbf{x}_1 incorrectly. Given the value of λ in grid search, the base strong rule (Tibshirani et al., 2012) and the safe rule (Ghaoui et al., 2010) for lasso purge any selected variable that satisfies, respectively, (2.4) and (2.5):

$$|\mathbf{x}_i^T Y| < \lambda - \|\mathbf{x}_i\|_2 \|Y\|_2 \frac{\lambda_{max} - \lambda}{\lambda_{max}}; \quad (2.4)$$

$$|\mathbf{x}_i^T Y| < 2\lambda - \lambda_{max}, \quad (2.5)$$

where the \mathbf{x}_i are standardized and λ_{max} is the value of λ that purges all the variables in coordinate descent optimization. Both rules are based on the marginal covariance between

\mathbf{x}_i and Y . For a given value of λ (typically selected by CV), lasso likely will select \mathbf{x}_1 and \mathbf{x}_2 along with some redundant variables from $\{\mathbf{x}_3, \dots, \mathbf{x}_{99}\}$ (since the DGP does not violate any IRC). Since $\text{corr}(\mathbf{x}_1, Y) = \text{corr}(\mathbf{x}_3, Y) = \dots = \text{corr}(\mathbf{x}_{99}, Y) = 0$ in the population, the sample value of $|\mathbf{x}_1^T Y|$ will be approximately as small as the $|\mathbf{x}_i^T Y|$ of any redundant variable. Put another way, \mathbf{x}_1 cannot be distinguished from the redundant variables by the value of $|\mathbf{x}_i^T Y|$. To ensure \mathbf{x}_1 is not purged by (2.4) or (2.5), both $\lambda - \|\mathbf{x}_1\|_2 \|Y\|_2 \frac{\lambda_{max} - \lambda}{\lambda_{max}}$ and $2\lambda - \lambda_{max}$ must be smaller than $|\mathbf{x}_1^T Y|$. However, this will lead to two problems. First, decreasing the right-hand side of (2.4) and (2.5) will reduce the value of λ , implying that lasso will select more redundant variables. Second, since $|\mathbf{x}_1^T Y|$ will be approximately as small as the $|\mathbf{x}_i^T Y|$ of any redundant variable selected by lasso, not purging \mathbf{x}_1 (by reducing both right-hand side terms) may result in (2.4) and (2.5) retaining redundant variables.

Variable screening methods (Fan and Lv, 2008; Hall and Miller, 2009; Hall et al., 2009) may also be prone to selecting redundant variables. Screening ranks variables decreasingly based on the absolute values of their marginal correlations to Y , selecting the top w variables (with w selected by CV, bootstrap or BIC). Since $\text{corr}(\mathbf{x}_2, Y) \neq 0$ in the population, marginal correlation ranking will put \mathbf{x}_2 at the beginning of the ranking. However, it may not rank \mathbf{x}_1 highly because $\text{corr}(\mathbf{x}_1, Y) = 0$ in the population. Thus, some redundant variables may be ranked between \mathbf{x}_2 and \mathbf{x}_1 , implying that if both \mathbf{x}_1 and \mathbf{x}_2 are selected, screening will select redundant variables.

The average L_0 solution path will not suffer the same problem. For convenience, assume $-\alpha_1/\alpha_2 > 0$ and $p/n = 100/200$ or smaller. For lars, as we increase $\|\beta_2\|_1$ at stage 1 (i.e., as we ‘partial’ \mathbf{x}_2 out of Y), the marginal correlation between $Y - \beta_2 \mathbf{x}_2$ and \mathbf{x}_1 will increase above 0 significantly while the marginal correlation between $Y - \beta_2 \mathbf{x}_2$ and any redundant variable will remain approximately 0. Thus, in the L_0 solution path and, hence, the average L_0 solution path, \mathbf{x}_1 will be included immediately after \mathbf{x}_2 is included. ■

In the second example we revisit Example 2, which illustrates another common scenario in empirical regression: *redundant variables* may be *marginally correlated to Y* in the DGP. In this example we choose specific values of β_1 , β_2 , ω and δ to demonstrate that, even when IRC is not violated, post-lasso selection rules and variable screening methods may have difficulty purging \mathbf{x}_3 (the sibling of Y). While forward regression is generally reliable, sensitivity may be an issue when n is small. By contrast, solar is more reliable, as will be shown in simulations 1 and 2.

Example 2 revisited. In Example 2, Y has two parents (informative variables) and a sibling (redundant variable). Due to the confounding structure, \mathbf{x}_1 , \mathbf{x}_2 and \mathbf{x}_3 are all marginally correlated to Y . Moreover, \mathbf{x}_3 is also marginally correlated to \mathbf{x}_1 and \mathbf{x}_2 . Consider a specific DGP for Example 2,

$$\begin{cases} \mathbf{x}_3 = \frac{1}{3}\mathbf{x}_1 + \frac{1}{3}\mathbf{x}_2 + \frac{\sqrt{7}}{3}u, \\ Y = \frac{7}{10}\mathbf{x}_1 + \frac{2}{10}\mathbf{x}_2 + \frac{\sqrt{47}}{10}e, \end{cases} \quad (2.6)$$

where \mathbf{x}_1 , \mathbf{x}_2 , u and e are independent; \mathbf{x}_3 is independent from e ; Y is independent from u ; and all variables are standardized. Thus, when n is large and the sample correlations close to the corresponding population values, the sample marginal correlations to Y can be ranked

in decreasing order,

$$\begin{aligned}\text{corr}(\mathbf{x}_1, Y) &= 0.7 \\ \text{corr}(\mathbf{x}_3, Y) &= \text{corr}\left(\frac{1}{3}\mathbf{x}_1 + \frac{1}{3}\mathbf{x}_2, \frac{7}{10}\mathbf{x}_1 + \frac{2}{10}\mathbf{x}_2\right) = 0.3. \\ \text{corr}(\mathbf{x}_2, Y) &= 0.2\end{aligned}\tag{2.7}$$

Thus, because \mathbf{x}_2 ranks below \mathbf{x}_1 and \mathbf{x}_3 in terms of marginal correlations to Y , the variable screening method will have to select all 3 variables, including the redundant variable \mathbf{x}_3 , to avoid omitting \mathbf{x}_2 .

Similarly, the base strong rule and safe rule may also have difficulty purging \mathbf{x}_3 . Because $\text{corr}(\mathbf{x}_3, Y)$ is larger than $\text{corr}(\mathbf{x}_2, Y)$, if lasso selects both \mathbf{x}_3 and \mathbf{x}_2 and we use the base strong rule or the safe rule to purge \mathbf{x}_3 , we will also purge \mathbf{x}_2 .

Forward regression and lars-lasso will not make the same error. Because (2.6) does not violate the IRC, variable-selection consistency of lars-lasso and forward regression is assured by the theoretical results of Zhang (2009) and Zhao and Yu (2006). Specifically in forward regression, \mathbf{x}_1 will be included at the first stage. After controlling for \mathbf{x}_1 , the partial correlations to Y of both \mathbf{x}_2 and \mathbf{x}_3 can be ranked in decreasing order as follows (when n is large),

$$\begin{aligned}\text{corr}(\mathbf{x}_2, Y|\mathbf{x}_1) &= \text{corr}\left(\mathbf{x}_2, \frac{2}{10}\mathbf{x}_2\right) = 0.2. \\ \text{corr}(\mathbf{x}_3, Y|\mathbf{x}_1) &= \text{corr}\left(\frac{1}{3}\mathbf{x}_1 + \frac{1}{3}\mathbf{x}_2, \frac{2}{10}\mathbf{x}_2\right) = 0.0667.\end{aligned}\tag{2.8}$$

Thus, at the second stage, forward regression will include \mathbf{x}_2 , not \mathbf{x}_3 . After controlling for both \mathbf{x}_1 and \mathbf{x}_2 , the remaining variation in Y comes from e , which \mathbf{x}_3 cannot explain. As a result, CV or BIC will terminate forward regression after the second stage and \mathbf{x}_3 will not be selected.

Despite their advantage over rank-based methods when n is large, lars-lasso and forward regression still suffer from sensitivity in high-dimensional spaces when n is small. By contrast, the average L_0 solution path based on \hat{q}_i reduces the sensitivity of forward regression to subsampling randomness, multicollinearity, noise and outliers. Simulation 3 below investigates in detail a similar dependence structure to (2.6). ■

The essential reason screening, the base strong rule and the safe rule struggle in these two examples is that they rely on the marginal correlations of variables to Y . By contrast, informative variables in regression analysis are defined in terms of conditional correlations. In many scenarios, marginal and conditional correlations are aligned. However, if the regression dependence structure deviates from the standard, variable selection based conditional correlation is able to select informative variables when selection based marginal correlation may not.

2.2. Subsample-ordered least-angle regression

The solar algorithm is based on Algorithm 2. It is summarized in Algorithm 3 and illustrated in Figure 7. Instead of the equiangular, partial-correlation search in least-angle regression,

Algorithm 3: Subsample-ordered least-angle regression (solar)

```

input :  $(Y, X)$ 
1 Randomly select 20% of the points in  $(Y, X)$  to be the validation set  $(Y_v, X_v)$ ; denote the
   remaining points  $(Y_r, X_r)$ ;
2 estimate  $\hat{q}$  using Algorithm 2 on  $(Y_r, X_r)$ ;
3 for  $c := 1$  to 0,  $stepsize = -0.02$  do
4   set  $Q(c) = \{\mathbf{x}_j \mid \hat{q}_j \geq c, \forall j\}$  and add all variables in  $Q(c)$  into an OLS model;
5   if sample size of  $(Y_r, X_r)$  is not less than  $|Q(c)|$  then
6     train the OLS model on  $(Y_r, X_r)$  and compute its validation error on  $(Y_v, X_v)$ ;
7   else
8     break the if-else statement and for loop
9   end
10 end
11 find  $c^*$ , the value of  $c$  associated with the minimal validation error on  $(Y_v, X_v)$ ; find  $Q(c^*)$ ;
12 (optional) start backward elimination on all variables in  $Q(c^*)$  using  $(Y, X)$  and redefine
    $Q(c^*)$  to be variables that survive backwards elimination;
13 return  $\hat{q}, \beta(Q(c^*), Y)$ 

```

variables are included into forward regression according to their order in the average L_0 solution path. Variables that are more likely to be informative will be included at earlier stages. Thus, variable selection is accomplished using the average L_0 solution path estimated in Algorithm 2. Note that the 20% validation set size at step 1 of the solar algorithm is based on heuristics of training-test splits in machine learning. Note also that the solar algorithm does not rely on validation per se: other methods such as Mallows's \mathcal{C}_p , BIC or AIC may be used.⁴

As illustrated in Figure 7, we use \hat{q} from Algorithm 2 to generate a list of variables $Q(c) = \{\mathbf{x}_j \mid \hat{q}_j \geq c, \forall j \leq p\}$. For any $c_1 > c_2$, $Q(c_1) \subset Q(c_2)$, implying there exists a sequence of nested sets $\{Q(c) \mid c = 1, 0.98, \dots, 0\}$. Each c denotes a stage of forward or least-angle regression. Thus, for a given value of c , $Q(c)$ denotes the set of variables with $\|\beta_i\|_0 = 1$ on average and $Q(c) - Q(c+0.02)$ is the set of variables with $\|\beta_i\|_0$ just turning to 1. Therefore, $\{Q(c) \mid c = 1, 0.98, \dots, 0\}$ is the average L_0 solution path of Definition 2.3. By reducing c in steps, Algorithm 3 includes variables according to their (decreasing) \hat{q}_j values. Validation is implemented to determine the optimal c , returning the variable list with the minimum validation error. At the end of Algorithm 3, the regression coefficient estimates on $Q(c^*)$ are returned. Backwards elimination, proposed by Zhang (2009) to improve the pruning accuracy of redundant variables, is available as an option in Algorithm 3.

The essence of Algorithm 3 is to conduct variable selection using the average L_0 solution path. In cases where L_1 -shrinkage is required (e.g., L_1 -shrunked kernel methods in reproducing kernel Hilbert spaces, including kernelized lasso and L_1 -penalty kernel logistic regression), we may modify Algorithm 3 slightly, yielding the *solars* algorithm summarized in Algorithm 4.

Algorithm 4 is a simple modification of lars-lasso. Lars-lasso includes variables stepwise

⁴We choose validation because it relies on fewer assumptions and can be applied to a wider range of models than BIC or AIC.

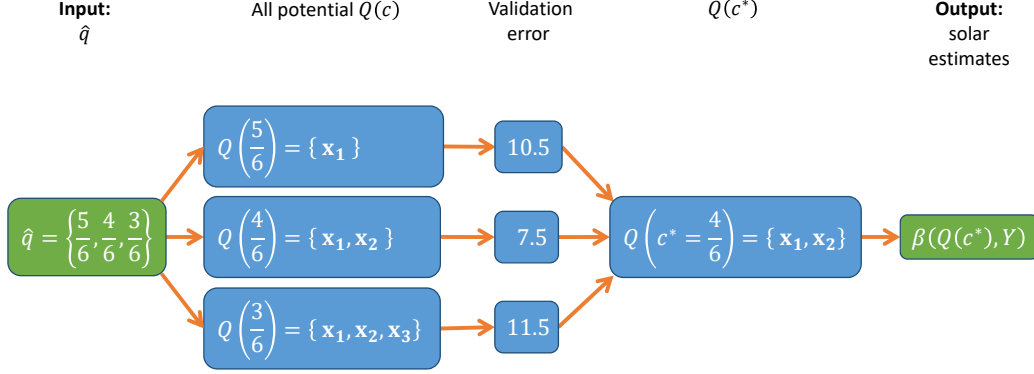


Fig 7: Computation flow for Algorithm 3 (continued from Figure 5).

into the solution path according to their partial correlations to Y . By contrast, Algorithm 4 partitions variables into groups $(Q(\hat{c}) - Q(\hat{c} + 0.02), \forall \hat{c} \in [0, 1])$ according to their positions in the average L_0 solution path. Variables in the same $Q(\hat{c}) - Q(\hat{c} + 0.02)$ are, on average, included by lars-lasso at the same stage. As a result, variables in the same $Q(\hat{c}) - Q(\hat{c} + 0.02)$ are added simultaneously in Algorithm 4.⁵

The aim of the Algorithm 4 modification is to increase tolerance to multicollinearity and non-standard dependence structures, with the goal of stabilizing solar(s) under harsh settings of the IRC. As shown in the simulations below, all the informative variables are listed at the beginning of the average L_0 solution path. Thus, informative variables are likely to be included at the very beginning of the loop between lines 4 and 6 of Algorithm 4. After all the informative variables have been included, the β_i of some redundant variables will begin to hit 0 repeatedly, as they would with lars-lasso, resulting in immediate elimination from the regression.

⁵This is similar to group lasso. The difference is that in group lasso all variables are manually grouped whereas in Algorithm 4 variables are grouped on the basis of the average L_0 solution path.

Algorithm 4: Subsample-ordered least-angle regression with shrinkage (solars)

```

input :  $(Y, X)$ 
1 Randomly select 20% of the points in  $(Y, X)$  to be the validation set  $(Y_v, X_v)$ ; denote the
   remaining points  $(Y_r, X_r)$ ;
2 estimate  $\hat{q}$  using Algorithm 2 on  $(Y_r, X_r)$ ; similar to Algorithm 3, obtain the average  $L_0$ 
   solution path  $\{Q(c)|c = 1, 0.98, \dots, 0\}$ 
3 Set  $\hat{c} := 1$ ;
   /* lars-lasso on the average  $L_0$  solution path starts here */
4 Add all variables in the set  $Q(\hat{c}) - Q(\hat{c} + 0.02)$  into regression model of  $Y$ ; increase their
   coefficient  $\beta_j$  in the direction of the sign of their correlation with  $Y$ ; take residuals  $\epsilon = Y - \hat{y}$ 
   along the way; drop any  $x_i$  with corresponding  $\beta_i$  hit 0 ;
5 stop line 4 when  $\max \{\text{corr}(\mathbf{x}_i, \epsilon) | \mathbf{x}_i \in Q(\hat{c}) - Q(\hat{c} + 0.02)\}$  is equal to
    $\max \{\text{corr}(\mathbf{x}_i, \epsilon) | \mathbf{x}_i \in Q(\hat{c} - 0.02) - Q(\hat{c})\}$ ;
6 Set  $\hat{c} := \hat{c} - 0.02$  and move back to line 4 until  $\hat{c} = 0$  or the number of variables in  $Q(\hat{c})$  equals
    $n$ ;
   /* lars-lasso on the average  $L_0$  solution path ends here */
7 Based on the  $L_1$  arc computed from line 4 to 6, use  $(Y_v, X_v)$  for validation to determine the
   optimal  $L_1$  shrinkage ratio  $t^*$  and corresponding regression coefficient  $\beta^*$ 
8 return  $t^*, \beta^*$ 

```

Discussion: effects of selection and shrinkage on the average L_0 solution path

Typically, lars-lasso is considered superior to forward regression in many applications. As Yuan and Lin (2007) shows, once a redundant variable is included by forward regression at stage l , it cannot be dropped at a subsequent stage. Suppose two informative variables \mathbf{x}_1 and \mathbf{x}_3 are included, respectively, at stage 1 and 3 and a redundant variable z is included at stage 2. To avoid forward regression mistakenly purging \mathbf{x}_3 , z will be retained in the final regression model. By contrast, a (redundant) variable included at stage l in the lars-lasso solution path may be dropped when its regression coefficient hits 0 in following stages. Thus, lars-lasso is less prone than forward regression to selecting redundant variables.

Nevertheless, the L_1 arch of lars-lasso and the forward regression solution path may not be robust to sampling randomness or multicollinearity in high-dimensional data. As a result, redundant variables may be included at early stages in the lars-lasso solution path. By contrast, the simulations below repeatedly show that the average L_0 solution path in solar is more likely to include informative variables before redundant variables. Hence, by computing the average L_0 solution path, solar is more robust to sampling randomness and multicollinearity. In simulations 1-3 below using a given high-dimensional data set we show that, compared with lars-lasso, solar is more accurate and robust in terms of distinguishing informative variables from redundant variables.

Solar(s) has several other advantages. First, it solves Example 1 type problems. Solar(s) relies on a single, average L_0 solution path ($\{Q(c)|c = 1, 0.98, \dots, 0\}$) and a fixed training-validation split to determine c^* for solar (t^* for solars). As a result, on the average L_0 solution path, each value of c is mapped to a unique set of selected variables and each value of t is uniquely mapped to a given shrinkage amount. Second, given a standard dependence

structure, because each value of t is uniquely mapped to a value of λ (computable under Kuhn-Tucker conditions), we can apply post-lasso selection rules to the Algorithm 4 results. Third, since the average L_0 solution path gives Algorithms 3 and 4 additional robustness against subsampling randomness, multicollinearity, noise and outliers in high-dimensional spaces, post-estimation statistical tests (for either lars-lasso or forward regression) on Algorithm 3 and 4 results are more appropriate. Last but not least, both solar and solars are computationally efficient (see section 3.1).

Owing to their flexibility, solar and solars may be generalized to a range of statistical problems, although which application is suitable depends on the research setting. Solar (selection without shrinkage) and solars (selection with shrinkage) are both well-suited to classical linear regression. However, differences in the way variables are selected in the two algorithms highlights an important feature of Algorithm 3. Solar may be thought of as ‘selective shrinkage’: the β_i of the selected variables are free from shrinkage while the β_j of the eliminated variables are shrunked directly to 0. Thus, Algorithm 3 retains a property called ‘probabilistic unbiasedness’ (similar to the Meinshausen (2007) result for relaxed lasso) that Algorithm 4 does not: with a large probability, a solar regression coefficient is unbiased (as shown in simulations 1, 2 and 3). Partially due to this property, we choose solar for the simulations and do not consider Algorithm 4 further.

3. Subsample-ordered least-angle regression: computation

In this section, we illustrate the computation of solar and discuss its computation load. The Python package `solarpy` for solar—coded in Python 3.7.3 (under Anaconda3 version 2019-03) on Debian 9.7 (equivalently, Ubuntu 18.04.2)—is contained in supplementary file B. The Python code is extensively documented with detailed comments and stepwise explanations.

3.1. Computation load

Since the computation load of least-angle regression on a given sample is fixed, we may use the number of least-angle regressions required by solar and K -fold, cross-validated least-angle regression for lasso (CV-lars-lasso) to approximate the respective computation loads. For comparison purposes, we compute solar with K subsamples and CV-lars-lasso with K -fold cross-validation.⁶ As shown in Algorithm 2, we need to compute one unconstrained lars for solar on each subsample (X^k, Y^k) , implying we need to estimate K unconstrained lars to compute \hat{q} (assuming we ignore the backwards-elimination option in Algorithm 3) and one to compute c^* . CV-lars-lasso requires computing K lars to optimize the tuning parameter t and, given the optimal tuning parameter, one lars on the full sample to select variables. Thus, the computation load for solar is roughly the same as for CV-lars-lasso. Since solar is shown to be more sparse, stable and accurate in terms of variable selection than CV-lars-lasso

⁶Some lasso modifications (e.g., fused lasso, grouped lasso) are designed to solve specific empirical problems (e.g., spatial autocorrelation or dummy variable issues) that are not relevant to our paper. Moreover, it may be difficult to investigate by how much other lasso variants outperform lasso. For example, while Jia and Yu (2010) show numerically that elastic net has a slightly better variable-selection accuracy than lasso, they also find that “when the lasso does not select the true model, it is more likely that the elastic net does not select the true model either.” Hence, we focus on the comparison between lasso and solar.

(sections 4.1-4.3), matching the computation load of CV-lars-lasso is an important attribute of solar. It is harder to compare the computation loads for lars-lasso and coordinate descent. Lars-lasso optimizes t in one training round; coordinate descent needs to be recomputed for each value of λ in grid search. Hence, lars-lasso may require less computation than coordinate descent in some data sets and more in others.

3.2. Solar computation

To demonstrate the step-by-step computation of solar, the data generating process (DGP) is specified as follows. The response variable $Y \in \mathbb{R}^{n \times 1}$ is generated by

$$Y = X\beta + e = 2\mathbf{x}_0 + 3\mathbf{x}_1 + 4\mathbf{x}_2 + 5\mathbf{x}_3 + 6\mathbf{x}_4 + e \quad (3.1)$$

where $X \in \mathbb{R}^{n \times p}$ is generated from a zero-mean, multivariate Gaussian distribution with covariance matrix with 1 on the main diagonal and 0.5 for the off-diagonal elements. All data points are identically and independently distributed. Each \mathbf{x}_j is independent from the noise term e , which is standard Gaussian. Initially we set $n = 200$ and $p = 100$.

In this simulation, we first generate the sample (Y, X) . For solar, we randomly reserve 20% of the points in (Y, X) as the validation set (denoted as (Y_v, X_v) in Algorithm 3) and use the remaining 80% (denoted as (Y_r, X_r) in Algorithm 3) to generate subsamples. Each subsample is generated by randomly removing 10% of the points in (Y_r, X_r) . Solar competes with K -fold, cross-validated lars-lasso (CV-lars-lasso) and K -fold, cross-validated pathwise cyclic coordinate descent with warm starts (CV-cd) estimated on (Y, X) . CV-lars-lasso and CV-cd are both from the `Sci-kit learn` library—a Google open-source machine-learning Python package by [Pedregosa et al. \(2011\)](#). We choose the number of CV folds and the number of subsamples generated in Algorithm 2 to be 10, following the [Friedman et al. \(2001\)](#) simulations that show $K = 10$ balances the bias-variance trade-off in CV error minimization.

Table 1 lists the variables selected by solar, CV-lars-lasso and CV-cd in this simulation.

TABLE 1
Variables selected by solar, CV-lars-lasso and CV-cd in the initial simulation.

| | Variables selected (listed in order of selection) | Total |
|---------------|--|-------|
| solar | $\mathbf{x}_4, \mathbf{x}_3, \mathbf{x}_2, \mathbf{x}_1, \mathbf{x}_0$ | 5 |
| CV-lars-lasso | $\mathbf{x}_4, \mathbf{x}_3, \mathbf{x}_2, \mathbf{x}_1, \mathbf{x}_0, \mathbf{x}_{71}, \mathbf{x}_{91}, \mathbf{x}_{90}, \mathbf{x}_{17}, \mathbf{x}_{40}, \mathbf{x}_{70}, \mathbf{x}_{65}, \mathbf{x}_{94}, \mathbf{x}_{28}$ | 14 |
| CV-cd | $\mathbf{x}_4, \mathbf{x}_3, \mathbf{x}_2, \mathbf{x}_1, \mathbf{x}_0, \mathbf{x}_{71}, \mathbf{x}_{91}, \mathbf{x}_{90}, \mathbf{x}_{17}, \mathbf{x}_{40}, \mathbf{x}_{70}, \mathbf{x}_{65}, \mathbf{x}_{94}, \mathbf{x}_{28}, \mathbf{x}_{19}, \mathbf{x}_{31}, \mathbf{x}_{41}$ | 17 |

Table 1 shows that solar successfully selects all the informative variables and drops all the redundant variables. The performance of CV-lars-lasso and CV-cd is similar though inferior to solar: CV-lars-lasso selects 9 redundant variables and CV-cd selects 12 variables

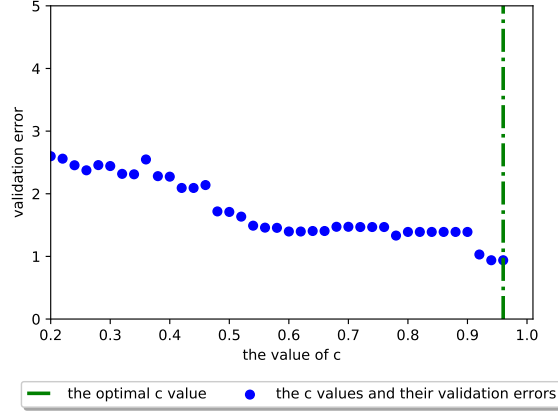
Fig 8: Tuning c using validation.

Figure 8 shows the solar tuning procedure for c : the path to c^* that minimizes the validation error. In this case, $c^* = 0.955$ returns the minimum validation error, implying the list of selected variables $\{\mathbf{x}_j \mid \hat{q}_j \geq 0.955\}$ (the validation errors of $c > 0.955$ are well over 5 and hence not plotted in Figure 8).

TABLE 2
Variables in $Q(c) = \{\mathbf{x}_j \mid \hat{q}_j \geq c\}$ (c^* in red)

| c | Variables in $Q(c)$ |
|-------|--|
| 1 | $\{\mathbf{x}_4\}$ |
| 0.977 | $\{\mathbf{x}_4, \mathbf{x}_3, \mathbf{x}_2\}$ |
| 0.955 | $\{\mathbf{x}_4, \mathbf{x}_3, \mathbf{x}_2, \mathbf{x}_1, \mathbf{x}_0\}$ |
| 0.911 | $\{\mathbf{x}_4, \mathbf{x}_3, \mathbf{x}_2, \mathbf{x}_1, \mathbf{x}_0, \mathbf{x}_{19}\}$ |
| 0.888 | $\{\mathbf{x}_4, \mathbf{x}_3, \mathbf{x}_2, \mathbf{x}_1, \mathbf{x}_0, \mathbf{x}_{19}, \mathbf{x}_{68}, \mathbf{x}_{40}, \mathbf{x}_{18}\}$ |
| 0.755 | $\{\mathbf{x}_4, \mathbf{x}_3, \mathbf{x}_2, \mathbf{x}_1, \mathbf{x}_0, \mathbf{x}_{19}, \mathbf{x}_{68}, \mathbf{x}_{40}, \mathbf{x}_{18}, \mathbf{x}_{91}, \mathbf{x}_{71}\}$ |

Table 2 shows c^* and the optimal variable group $Q(c^*)$ highlighted in red, confirming that only the first five variables are selected by solar. As shown in Table 1, while CV-lars-lasso and CV-cd select the first five (informative) variables they also select a number of additional (redundant) variables. Thus, solar has an advantage in terms of sparsity.

Table 2 also reveals an interesting feature of solar. As Lockhart et al. (2014) shows, testing significance with the lasso is not straightforward due to L_1 shrinkage and other lasso attributes. By contrast, solar is a forward regression on the average L_0 solution path. Since the average L_0 solution path is nested and since solar is free from shrinkage, it is straightforward to verify statistical significance of solar variable-selection results. For example, suppose in the Table 2 results we are concerned that solar has wrongly included $\{\mathbf{x}_1, \mathbf{x}_0\}$. To investigate, we may simply set up a χ^2 -test with

$$\begin{aligned}
H_0 : \bar{\beta}_0 &= \bar{\beta}_1 = 0; \\
H_1 : \bar{\beta}_j &\neq 0 \text{ for at least one of } j = 0, 1,
\end{aligned}$$

where $\bar{\beta}_j$ is the population value of β_j .

4. Subsample-ordered least-angle regression: simulations

In this section, we use simulations to compare the variable-selection performance of solar, CV-lars-lasso and CV-cd in a variety of settings. We use four criteria for comparison: sparsity, stability, accuracy and robustness. Sparsity is measured by the number of variables selected. Stability is evaluated by the median and range of the distribution of the number of variables selected. Accuracy is measured by the incidence of type-I and type-II errors in variable selection defined as follows.

Definition 4.1 (Type-I and Type-II errors in variable selection).

1. If \mathbf{x}_j is a **redundant** variable that is **selected** by the variable-selection estimator, the estimator commits a type-I variable-selection error on \mathbf{x}_j (denoted $\text{VSE-I}(\mathbf{x}_j)$).
2. If \mathbf{x}_j is an **informative** variable that is **not selected** by the variable-selection estimator, the estimator commits a type-II variable-selection error on \mathbf{x}_j (denoted $\text{VSE-II}(\mathbf{x}_j)$).

Lastly, robustness is measured by the impact on sparsity, stability and accuracy of changes in the irrerepresentable condition (IRC).

The DGP for the simulations is the same as (3.1). We carry out 4 simulations (each with 200 repeats and fixed random seeds) to compare the performance of solar, CV-lars-lasso and CV-cd using the same (X, Y) data set. In simulation 1, we assess convergence for solar, CV-lars-lasso and CV-cd for $p = 100$ as the sample size n increases (i.e., when p/n slowly approaches 0 from above). Next, we compare the performance of solar, CV-lars-lasso and CV-cd in high-dimensional spaces. In simulation 2a, p/n slowly approaches 1 from above, and in simulation 2b, p/n remains constant as both n and p increase rapidly. In simulation 3, we compare the performance of solar, CV-lars-lasso and CV-cd under different settings of the irrerepresentable condition when $p/n = 50/200$. The full set of simulation results are available in supplementary file C.

4.1. Simulation 1: effect of sample size

Simulation 1 compares performance when $p = 100$ and sample size increases from 50 to 100 and 200. We find that solar tends to converge to (3.1) in terms of selected variables (Table 3, Figures 10 and 11) and accuracy of the regression coefficients (Figure 12). As p/n decreases, CV-lars-lasso and CV-cd also tend to converge to (3.1), although more slowly than solar. Overall, we find that solar is more responsive to decreases in p/n than CV-lars-lasso and CV-cd.

Sparsity and stability comparison

Figure 9 shows histograms of the number of variables selected by solar, CV-lars-lasso and CV-cd from the 200 simulations. When $p/n = 100/50$, the Figure 9a and 9d histogram for solar is right-skewed, with a median of 9.5, compared with the more symmetric CV-lars-lasso and CV-cd histograms, which have medians of 18. When p/n falls to 100/100, the Figure 9b and 9e solar histograms display thinner tails and a more prominent mode than CV-lars-lasso and CV-cd. When p/n falls to 100/200, Figures 9c and 9f show a more conspicuous difference between solar and its competitors. The mean for solar is just over 7.58, its median drops to

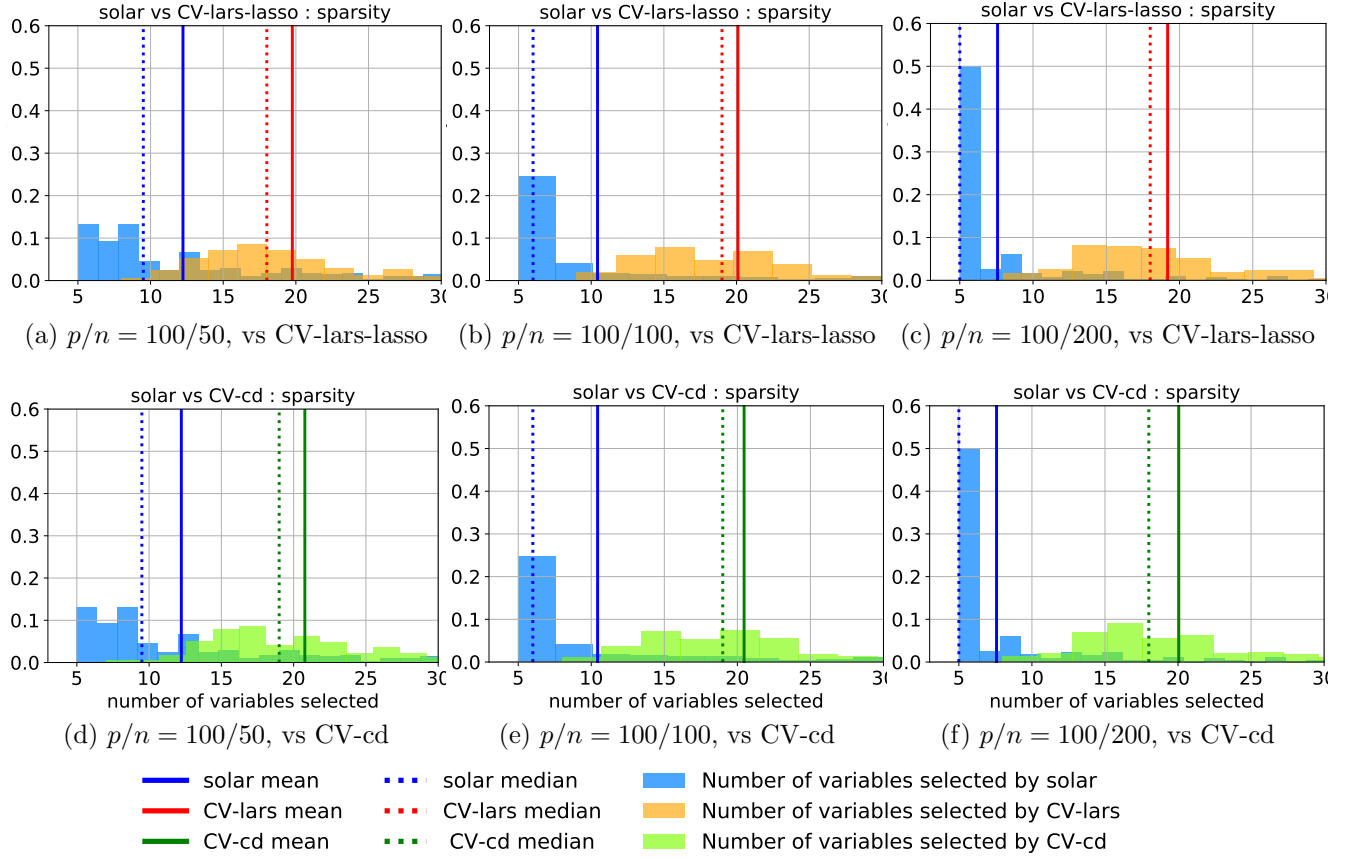


Fig 9: Histogram of the number of variables selected in simulation 1: solar vs competitors.

5, the mode density rises and the right tail of the histogram becomes thinner. By contrast, the medians for CV-lars-lasso and CV-cd decrease to 18 and the distributions shift slightly to the left. Overall, solar is more sparse than CV-lars-lasso in terms of variable selection.

Table 3 summarizes the mean and median values of the number of variables selected in Figure 9. The $p/n = 100/50$ case corresponds to a high-dimensional data variable-selection problem. In this case, on average, CV-cd and CV-lars-lasso both select around 20 variables and solar selects 12.33 variables, roughly 7 fewer. When n increases to 100, the mean and median number of variables selected by solar decrease, the values for CV-lars-lasso actually increase slightly, while the mean for CV-cd decreases and its median is unchanged from $n = 50$. When n increases to 200, all three algorithms improve performance in terms of sparsity, although both CV-lars-lasso and CV-cd select at least 10 more variables than solar.

Comparison of variable-selection accuracy

Given the DGP, Definition 4.1 states that an estimator that selects any of $\{\mathbf{x}_5, \dots, \mathbf{x}_{99}\}$ commits a VSE-I while an estimator that drops any of $\{\mathbf{x}_0, \dots, \mathbf{x}_4\}$ commits a VSE-II. Ideally, all 5 informative variables would be selected and all 95 redundant variables would be dropped. Figure 10 shows the probabilities redundant variables are selected for the 15 variables with the highest probabilities. For CV-lars-lasso and CV-cd, Figures 10a and 10d

TABLE 3
Number of variables selected in simulation 1.

| | | p/n | | |
|---|---------------|--------|---------|---------|
| | | 100/50 | 100/100 | 100/200 |
| mean | solar | 12.33 | 10.43 | 7.58 |
| | CV-lars-lasso | 19.75 | 20.09 | 19.19 |
| | CV-cd | 20.77 | 20.46 | 20.00 |
| median | solar | 9.5 | 6 | 5 |
| | CV-lars-lasso | 18 | 19 | 18 |
| | CV-cd | 18 | 19 | 18 |
| Pr(only select $\{\mathbf{x}_0, \mathbf{x}_1, \mathbf{x}_2, \mathbf{x}_3, \mathbf{x}_4\}$) | solar | 0.025 | 0.305 | 0.560 |
| | CV-lars-lasso | 0 | 0 | 0 |
| | CV-cd | 0 | 0 | 0 |

show the redundant variables \mathbf{x}_{75} and \mathbf{x}_{50} appear in the top-3 largest VSE-I probabilities (over 0.2) while the remaining 14 variables have similar VSE-I probabilities. By contrast, the VSE-I probabilities for solar in Figure 10a are about half the CV-lars-lasso and CV-cd values.

When n increases to 100 in Figure 10h, the VSE-I probabilities for solar decrease for all the variables. However, there is no decline in the CV-lars-lasso and CV-cd VSE-I probabilities (Figures 10b and 10e). Likewise, as n increases to 200, Figure 10i shows the VSE-I probabilities for solar decrease further while there is no clear improvement for CV-lars-lasso or CV-cd. Consistent with Figures 9a-9c, the VSE-I probabilities fall more rapidly for solar than for CV-lars-lasso and CV-cd as n increases from 50 to 200.

Figure 11 shows the probabilities that the 5 informative variables are selected in simulation 1. In each case, solar, CV-cd and CV-lars-lasso select $\{\mathbf{x}_2, \mathbf{x}_3, \mathbf{x}_4\}$ in all 200 simulations, implying that no estimator commits a VSE-II on $\{\mathbf{x}_2, \mathbf{x}_3, \mathbf{x}_4\}$. When $p/n = 100/50$, solar commits a VSE-II on \mathbf{x}_0 with 5% probability and \mathbf{x}_1 with 0.5% probability (see supplementary file C for detail). The solar VSE-IIs disappear for $n > 50$.

Across both types of variable selection error, solar largely retains all of the informative variables and, on average, drops a larger number of redundant variables, reinforcing the superior sparsity performance of solar noted above. Table 3 displays the probabilities solar, CV-lars-lasso and CV-cd avoid both VSE-I and VSE-II, referred to as the *VSE-free probability*. While the VSE-free probability for solar increases quickly as p/n decreases, it remains at 0 for CV-lars-lasso and CV-cd at all values of p/n .

Given the stability issue raised in Example 1, it is perhaps not surprising that CV-lars-lasso shows little improvement as p/n falls to 100/200. Simulation 3 below shows that there is a substantial improvement with CV-lars-lasso and CV-cd when p/n decreases further to 50/200 (Figure 19a, 19d, 20a, 20d, 21a and 21d). This is consistent with Example 1 and Lim and Yu (2016). When $p/n > 1$, both CV-lars-lasso and CV-cd may encounter variable-selection stability problems. However, as p/n falls below 1, the problems gradually disappear as n increases. In other words, while CV-lars-lasso and CV-cd exhibit a tendency to converge to the population model, it is a weaker tendency than solar. Hence, we conclude that solar is overall more responsive to decreases in p/n in high-dimensional spaces.

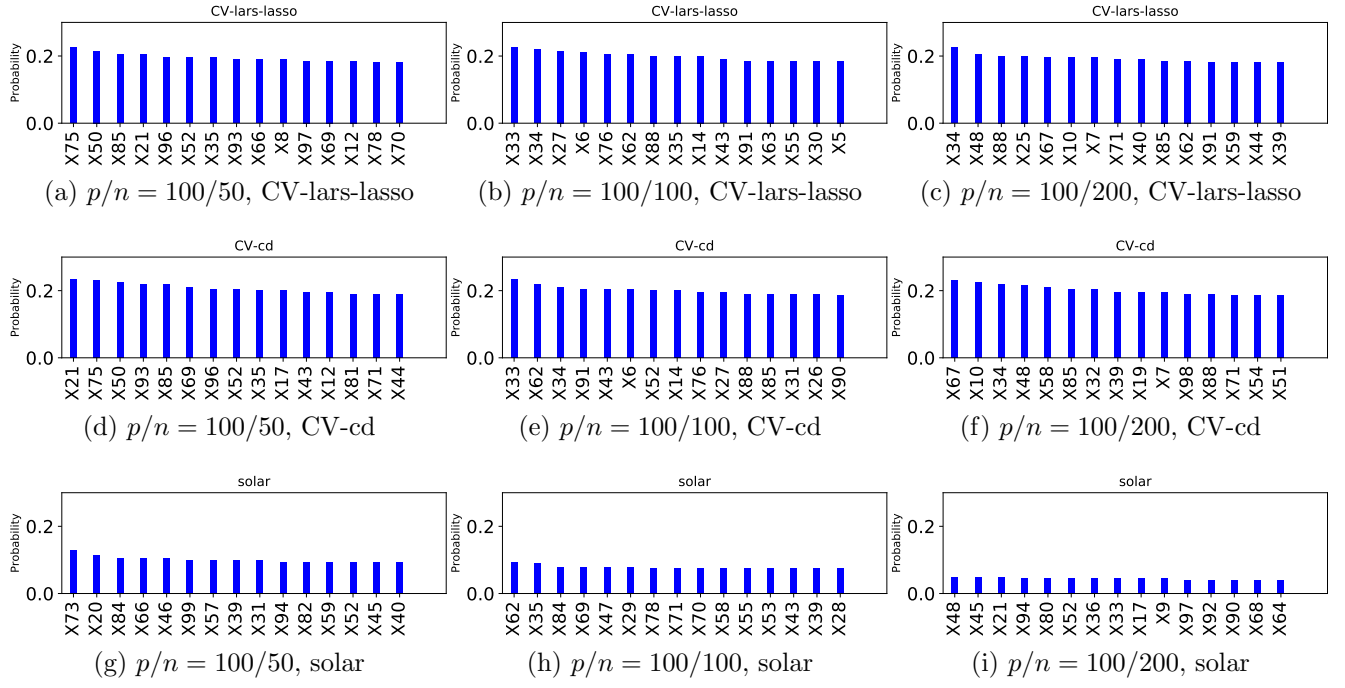


Fig 10: Probability of selecting redundant variables in simulation 1 (top 15 by probability).

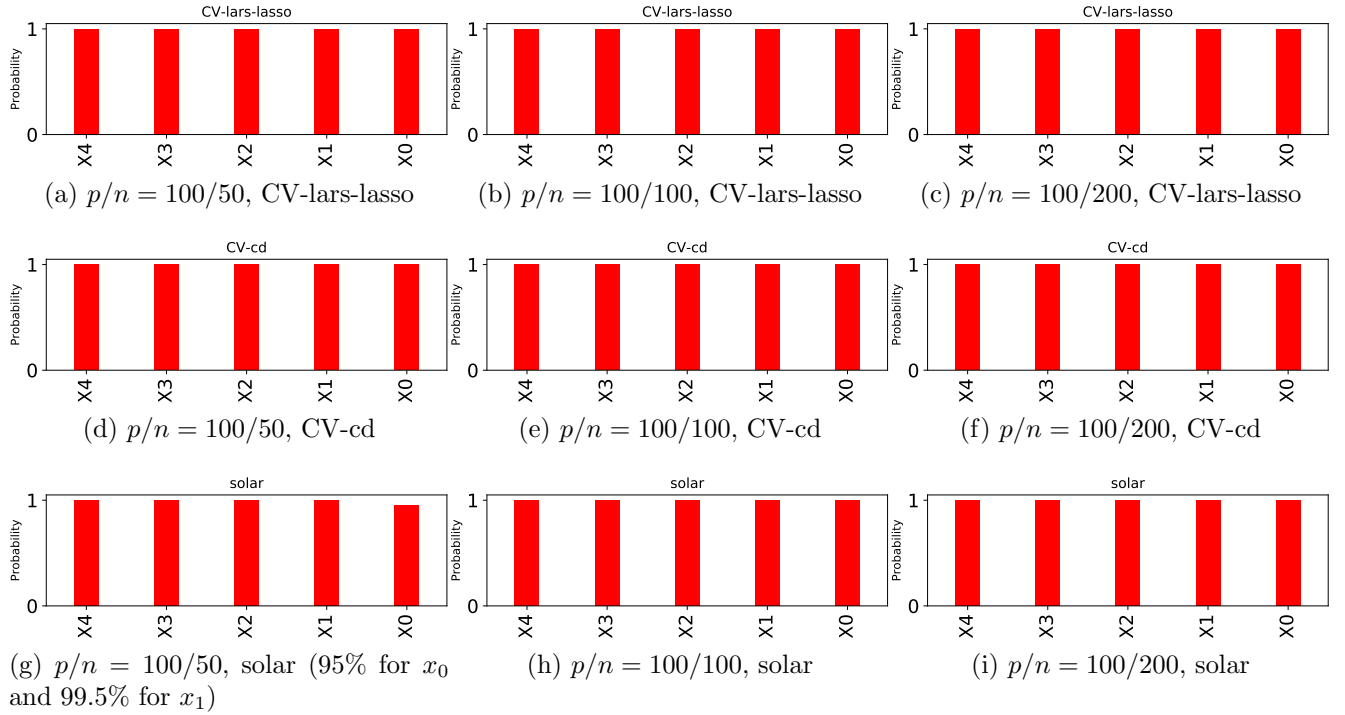


Fig 11: Probability of selecting informative variables in simulation 1.

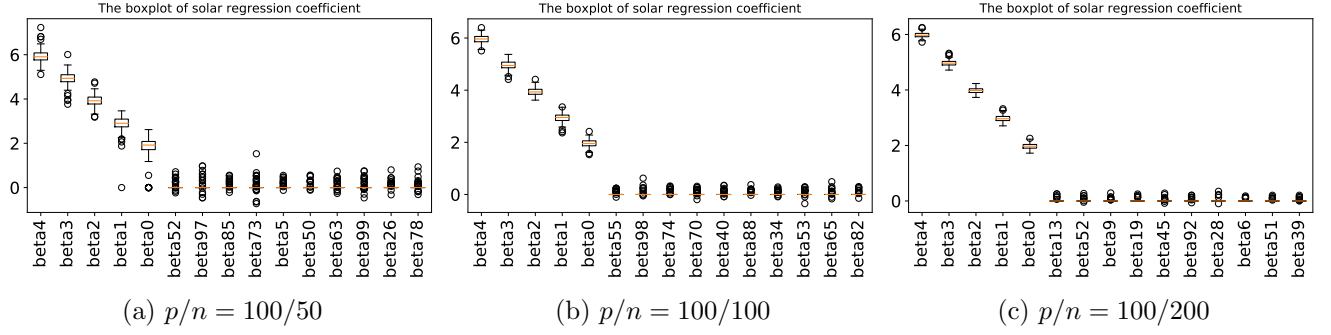


Fig 12: Solar regression coefficient boxplots in simulation 1 (top 15 by mean).

Solar regression coefficient boxplots

The third property we investigate is the stability of the solar coefficient estimates. Since there are 100 regression coefficients, we report only the top 15 (by mean) coefficient boxplots across the 200 repeats. The Figure 12 boxplots clearly show a tendency for L_2 consistency: the boxplots for each solar regression coefficient become more concentrated around the corresponding population values as n increases from 50 to 200.

Figure 12 also illustrates an interesting attribute of solar, which we refer to as *probabilistic unbiasedness*. Solar regression coefficients are estimated by OLS on the support pre-selected by Algorithms 2 and 3. OLS coefficient estimates are unbiased under regularity conditions and when all the informative variables are selected. Figure 10 shows that the probabilities solar includes redundant variables decrease rapidly as n increases. Figure 11 shows that the probabilities solar includes informative variables are 100% for $p/n = 100/100$ and $100/200$. Table 3 shows that the VSE-free probability for solar also increases rapidly. Thus, solar regression coefficients should be unbiased with probability 100% when p/n is $100/100$ and $100/200$ and with probability 95% when p/n is $100/50$. Figure 12 verifies this conjecture. When p/n is $100/50$, the β_0 boxplot has 10 outliers at 0 while the β_1 boxplot has only one. For the β_0 to β_4 boxplots when $p/n = 100/50$, some of the medians are slightly below the true values and some of the inter-quartile ranges are not perfectly symmetric around the true values in the DGP (due to solar omitting \mathbf{x}_0 or \mathbf{x}_1 with probability 5%). When p/n decreases to $100/100$ and $100/200$, the first 5 variables are selected with probability 100% and the β_0 to β_4 boxplots are almost perfectly symmetric around the true values in the DGP.

Discussion: selection versus shrinkage in classical regression analysis

In addition to the advantages of using the average L_0 solution path, another advantage of solar over CV-lars-lasso is that it does not involve shrinkage. CV-lars-lasso performs variable selection by shrinking $\|\beta\|_1$, which is implemented by simultaneously shrinking each $\|\beta_j\|_1$, $\forall j \leq p$. Since $\|\beta_j\|_1$ of the informative variables is (presumably) larger than $\|\beta_j\|_1$ of the redundant variables, in principle there may exist an ‘ideal’ value of the shrinkage parameter (say λ^{**}) that selects the informative variables and drops all the redundant variables. However, CV may not be the best tool to find λ^{**} . Shrinkage in CV-lars-lasso has two opposing

effects on the CV error: shrinking $\|\beta_j\|_1$ of the redundant variables tends on average to reduce it, while shrinking $\|\beta_j\|_1$ of the informative variables tends on average to increase it. Minimizing the CV error implicitly involves a trade-off between the two effects. In particular, shrinkage will decrease the CV error if the former effect dominates (when λ is close to 0) and increase it if the latter effect dominates (when a moderate amount of shrinkage has already been applied to $\|\beta_j\|_1$ of the informative variables, causing the β_j of the informative variables to be significantly biased towards 0), which likely occurs when λ is close to but still less than λ^{**} . Hence, unless all the $\|\beta_i\|_1$ of the informative variables are considerably larger than the $\|\beta_i\|_1$ of the redundant variables, CV may choose a $\lambda < \lambda^{**}$ in a high-dimensional sample, resulting in a number of redundant variables being selected.

Solar avoids this problem because it does not simultaneously shrink the β_j , $\forall j \leq p$: once a variable is recognized to be informative, its regression coefficient is not subject to shrinkage. This avoids the CV-lars-lasso problem of ‘overshrinking’ the $\|\beta_j\|_1$ of the informative variables.⁷ Also, most of the time, \hat{q} places the informative variables at the beginning of the average L_0 solution path, resulting in better stability and accuracy in high-dimensional data. Both improvements imply that solar is more likely than CV-lars-lasso to select informative variables and drop redundant variables, effects that may be larger when $p > n$.

4.2. Simulation 2: effect of high-dimensional settings

With Example 1 in mind, simulation 2 investigates the stability and accuracy of solar, CV-lars-lasso and CV-cd when $p > n$. In simulation 2a, we start with $p = 150$ and $n = 50$ and change p/n to (slowly) approach 1 from 150/50 to 200/100 and 250/150. In this case, solar shows a steady improvement in terms of sparsity, accuracy and stability (Table 4, Figures 13, 14 and 15). By contrast, CV-lars-lasso and CV-cd fail to show any substantial improvement. In simulation 2b, we start with $p = 400$ and $n = 200$ and, keeping p/n constant, increase n and p quickly from 400/200 to 800/400 and 1200/600. In this case, the performance of CV-lars-lasso and CV-cd deteriorates rapidly across all criteria. The sparsity of solar deteriorates slowly (Table 5) while the boxplots of the solar regression coefficients demonstrate a small but steady improvement (a tendency to L_2 consistency). Overall, simulation 2 reveals that the advantages of solar over CV-lars-lasso and CV-cd are more pronounced in high dimensions.

4.2.1. Simulation 2a: small n ; p/n approaches 1

Sparsity and stability comparison

Figure 13 shows the histograms of the number of variables selected by solar, CV-cd and CV-lars-lasso by p/n . The solar histograms become more concentrated at the mode of 5 (the number of informative variables) as p/n changes from 150/50 to 250/150. By contrast, the histograms for CV-lars-lasso and CV-cd shift slightly rightwards as p/n approaches 1. Thus, the solar empirical distributions tend to improve, in contrast to the CV-cd and CV-lars-lasso distributions, which worsen. Again, solar demonstrates a clear advantage over CV-lars-lasso and CV-cd in terms of stability.

⁷For a similar reason, *solar* likely dominates *solars* for variable selection in classical regression analysis.

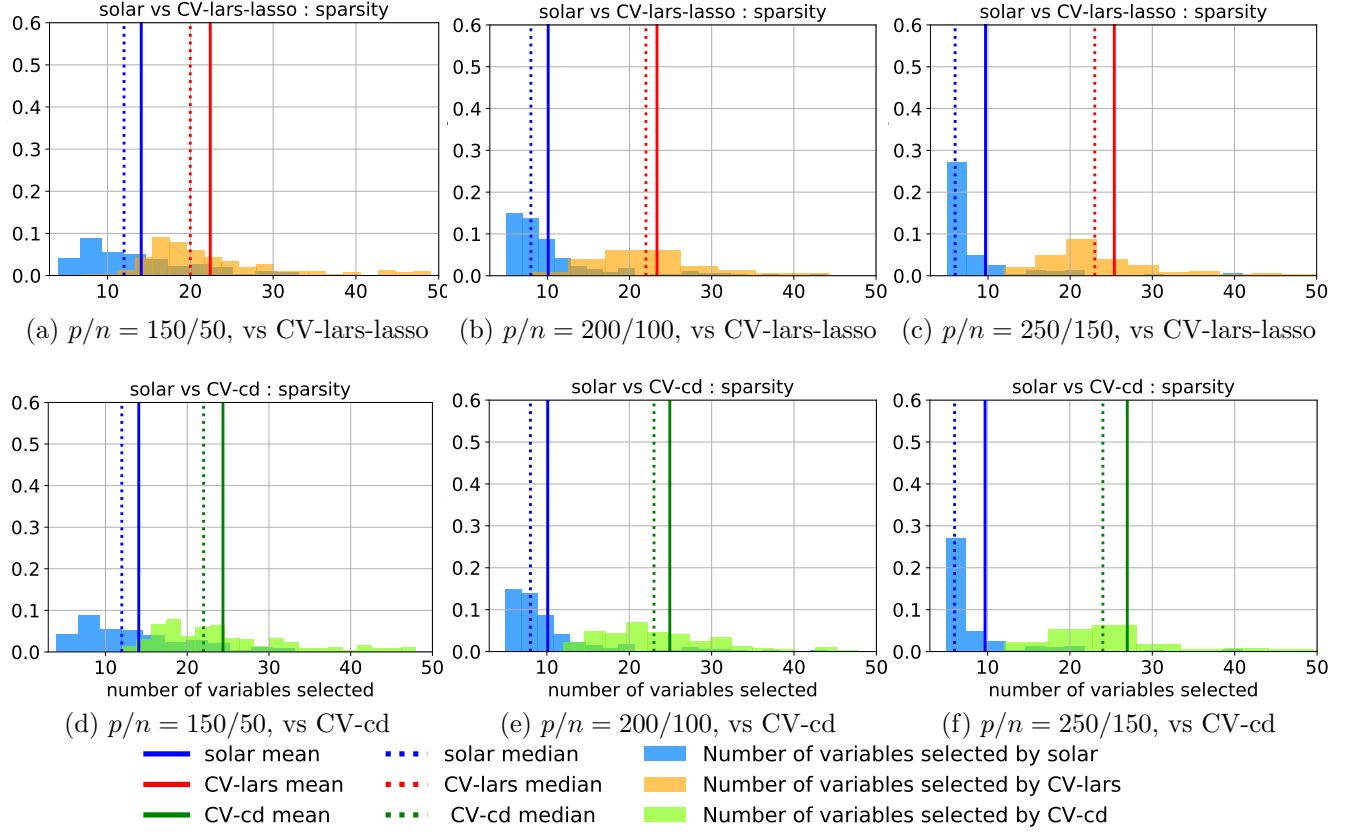


Fig 13: Histogram of the number of variables selected in simulation 2a.

TABLE 4
Number of variables selected in simulation 2a.

| | | p/n | | |
|---|---------------|--------|---------|---------|
| | | 150/50 | 200/100 | 250/150 |
| mean | solar | 14.07 | 10.10 | 9.7 |
| | CV-lars-lasso | 22.41 | 23.34 | 25.37 |
| | CV-cd | 24.37 | 24.92 | 26.96 |
| median | solar | 12 | 8 | 6 |
| | CV-lars-lasso | 20 | 22 | 23 |
| | CV-cd | 20 | 22 | 23 |
| Pr(only select $\{\mathbf{x}_0, \mathbf{x}_1, \mathbf{x}_2, \mathbf{x}_3, \mathbf{x}_4\}$) | solar | 0.015 | 0.115 | 0.445 |
| | CV-lars-lasso | 0 | 0 | 0 |
| | CV-cd | 0 | 0 | 0 |

Table 4 summarizes the information from the histograms, showing that CV-lars-lasso and CV-cd deteriorate while solar improves as p/n falls. When $p/n = 150/50$, solar on average selects at least 8 fewer variables than the competitors. When p/n falls to 200/100 and then to 250/150, the mean difference between solar and CV-lars-lasso and CV-cd actually increases, respectively, to 14 and 17.

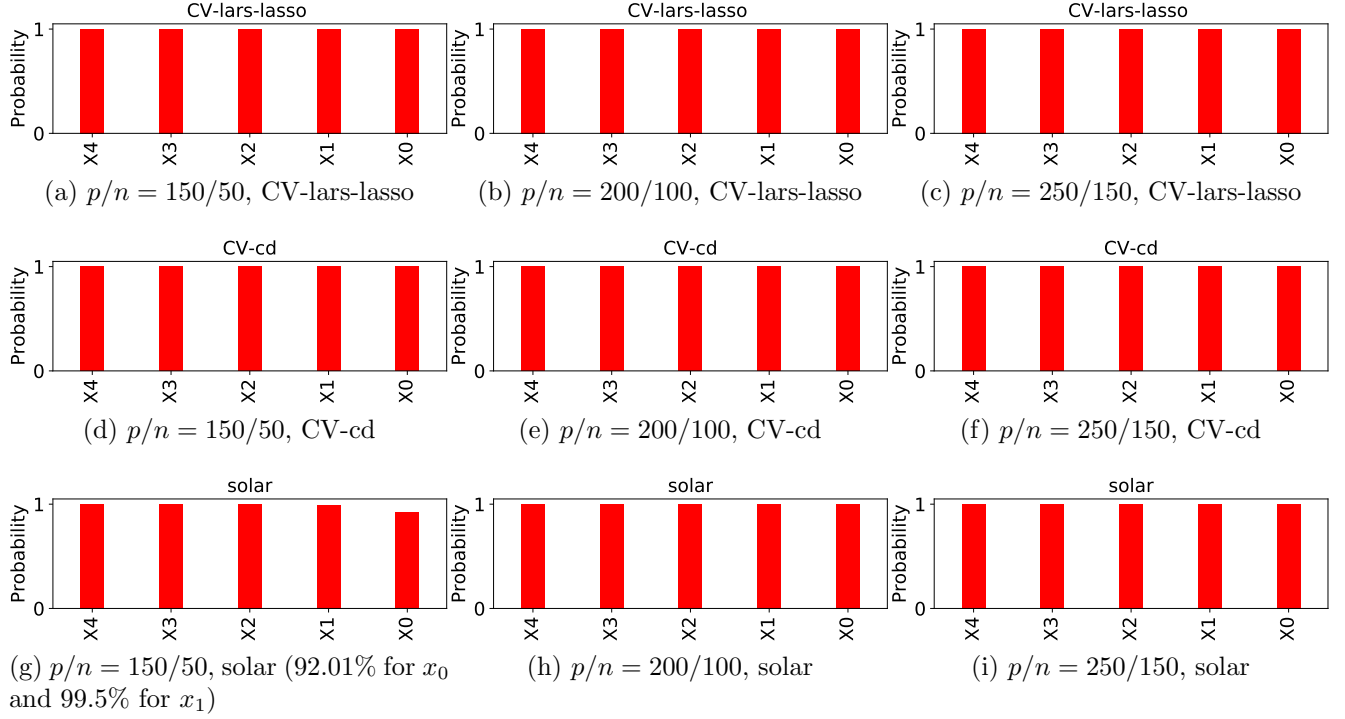


Fig 14: Probability of selecting informative variables in simulation 2a.

Comparing simulations 1 (Table 3) and 2a (Table 4) reveals another interesting property of solar. Compared to $p/n = 100/100$ in simulation 1, solar with $p/n = 200/100$ and $250/150$ on average is more sparse. In fact, the mean and median for solar with $p/n = 250/150$ is lower than for $p/n = 100/100$. On the other hand, the means and medians for CV-lars-lasso and CV-cd increase when p/n changes from $100/100$ to $200/100$ and $250/150$. Solar, CV-lars-lasso and CV-cd select all the informative variables with probability 1 when $p/n = 100/100$, $200/100$ and $250/150$ (Figure 11 in simulation 1 and Figure 15 in simulation 2a). Thus, given a small n , as p/n approaches 1, solar continues to improve in terms of sparsity and stability after CV-lars-lasso and CV-cd have stopped improving.

Comparison of variable-selection accuracy

The results in Figure 14 are similar to Figure 11 in simulation 1. CV-cd and CV-lars-lasso completely avoid any VSE-II while solar commits VSE-IIs only when $p/n = 150/50$ (on \mathbf{x}_0 with 7.99% probability and \mathbf{x}_1 with 0.05% probability).

Figure 15 shows that solar has substantially lower VSE-I probabilities than CV-lars-lasso and CV-cd. When $p/n = 150/50$, the (top 15) probabilities of a VSE-I for solar is around 0.1 compared with 0.2 for CV-lars-lasso and CV-cd. While the VSE-I probabilities for CV-lars-lasso and CV-cd decrease as p/n changes, the differences between solar and CV-lars-lasso increase as p/n changes from $200/100$ to $250/150$. It is also worth noting that the decrease in VSE-I probabilities for CV-lars-lasso and CV-cd do not help to improve variable-selection accuracy and sparsity (the means and medians increase in Table 4) because p increases so

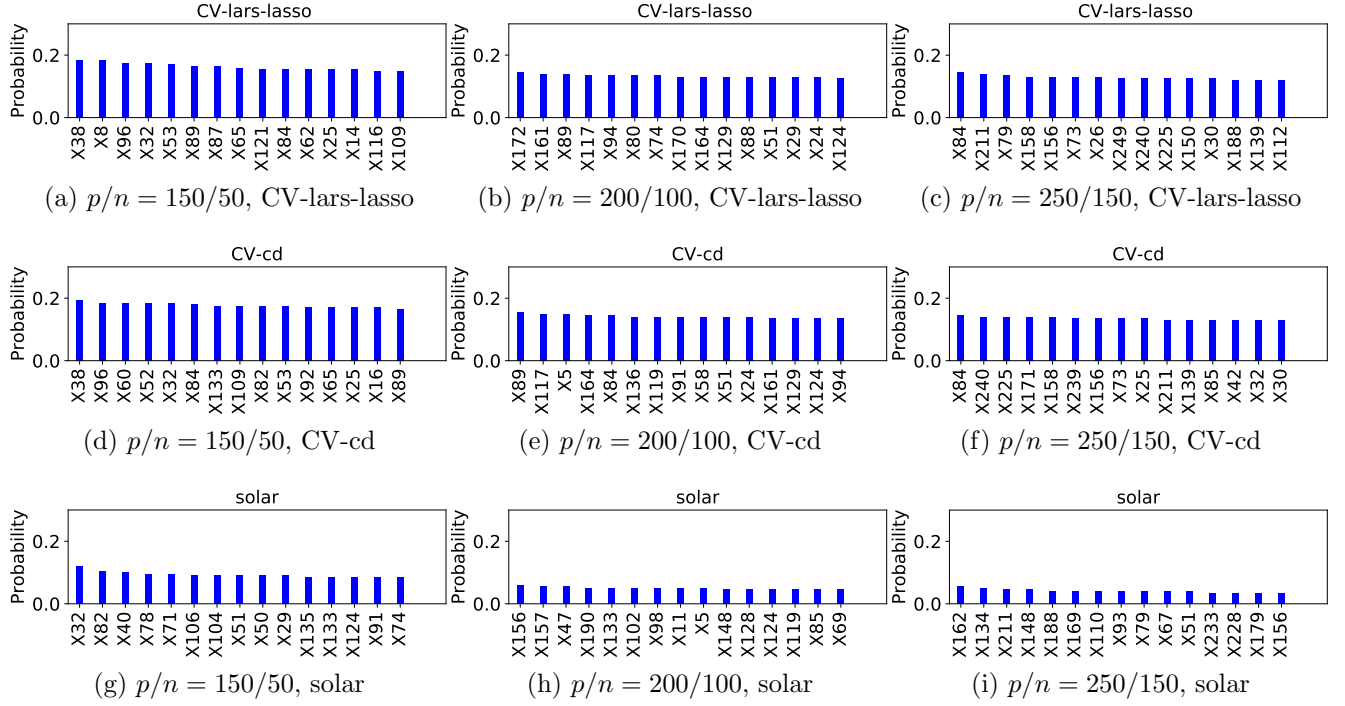


Fig 15: Probability of selecting redundant variables in simulation 2a (top 15 by probability).

rapidly in this simulation. On the other hand, the VSE-I probabilities approach 0 for solar, consistent with Figure 13.

Solar regression coefficient boxplots

The Figure 14 findings are confirmed in Figure 16. When $p/n = 150/50$, there are 16 outliers (black circles) for β_0 and one for β_1 at 0 while there are no outliers for β_2 , β_3 and β_4 . As p/n increases to 200/100 and 250/150, there are no outliers for β_0 or β_1 at 0. Meanwhile, the boxplots for each solar coefficient estimate become narrower and more symmetric as p/n changes, illustrating the same L_2 convergence tendency and probabilistic unbiasedness shown in Figure 12.

TABLE 5
Number of variables selected in simulation 2b.

| | | p/n | | |
|---|---------------|---------|---------|----------|
| | | 400/200 | 800/400 | 1200/600 |
| mean | solar | 10.88 | 13.80 | 14.85 |
| | CV-lars-lasso | 28.17 | 33.13 | 36.90 |
| | CV-cd | 29.58 | 35.07 | 38.76 |
| median | solar | 7 | 11 | 13 |
| | CV-lars-lasso | 26 | 31 | 33 |
| | CV-cd | 26 | 31 | 33 |
| $\Pr(\text{active set} = \{\mathbf{x}_0, \mathbf{x}_1, \mathbf{x}_2, \mathbf{x}_3, \mathbf{x}_4\})$ | solar | 0.150 | 0.010 | 0 |
| | CV-lars-lasso | 0 | 0 | 0 |
| | CV-cd | 0 | 0 | 0 |

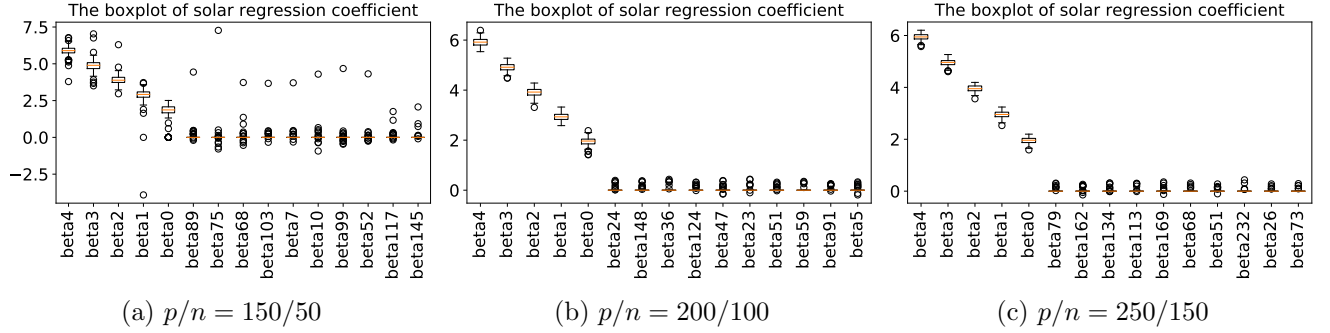


Fig 16: Solar regression coefficient boxplots in simulation 2a (top 15 by mean).

4.2.2. Simulation 2b: p and n increase rapidly; p/n remains constant

We report only the sparsity and stability comparison and the boxplots of the solar regression coefficients in this setting because the variable-selection accuracy results are similar to simulation 2a. The detailed results are available in supplementary file C. To summarize the accuracy results: none of the algorithms commit a VSE-I in any case while solar commits VSE-II with much lower probabilities than the competitors.

Sparsity and stability comparison

Table 5 shows that, as n and p increase rapidly, the sparsity of solar, CV-lars-lasso and CV-cd deteriorate, although solar outperforms the competitors. When p/n changes from 400/200 to 800/400, the means for CV-lars-lasso and CV-cd increase by 5 and 6 respectively, while the mean for solar increases by 3. The median number of variables selected for CV-lars-lasso and CV-cd increase by 5 while for solar the median increases by 4. Similar conclusions follow when p/n changes from 800/400 to 1200/600. Thus, solar also demonstrates a sparsity advantage over CV-lars-lasso and CV-cd in this setting.

Solar regression coefficient boxplots

The most interesting finding in simulation 2b is Figure 17: even though the sparsity of solar worsens, the boxplots of the solar regression coefficients actually improve. From Figure 17a to 17b and 17c, the boxplots become more concentrated around the true values and there are fewer outliers (black circles).

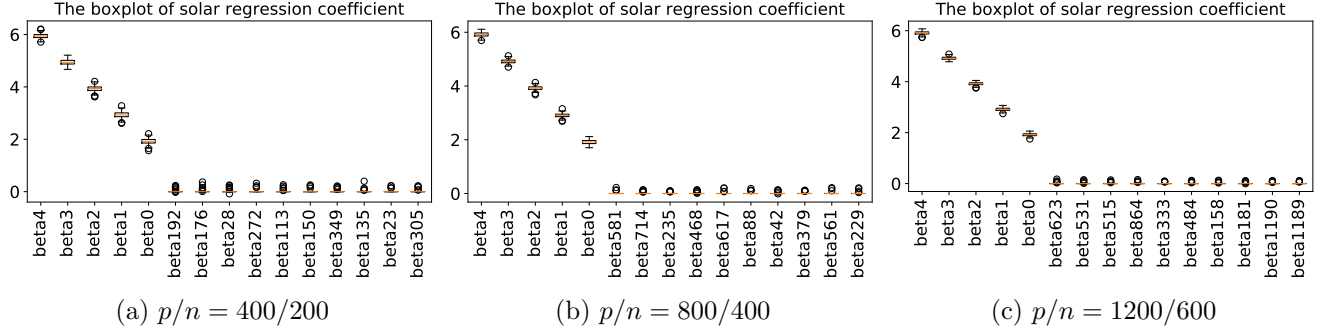


Fig 17: Solar regression coefficient boxplots in simulation 2 (top 15 by mean).

The reason for the improvement is as follows. Solar regression coefficients are computed by OLS of Y on $Q(c^*)$, the set of covariates selected by solar. Table 5 shows clearly that the average number of $|Q(c^*)|$ (the average number of variables selected by solar) only increases slightly as p/n changes. Computed by OLS, solar regression coefficients converge to the true values at the rate $\sqrt{|Q(c^*)|/n}$. Since $|Q(c^*)|$ increases only slightly when n increases by 200 from Figure 17a to 17b or Figure 17b to 17c and since $\{\mathbf{x}_0, \dots, \mathbf{x}_4\}$ remain jointly selected by solar, the boxplots become more concentrated around their true values. While regression coefficients from relaxed lasso share similar properties, solar is the better choice due to superior sparsity, stability, accuracy and its robustness to the irrerepresentable condition (shown in simulation 3).

4.3. Simulation 3: effect of different settings of the irrerepresentable condition

Keeping in mind Example 2 and the discussion in section 2.1, simulation 3 explores the robustness of solar, CV-lars-lasso and CV-cd to different settings of the IRC. Through simulation and theoretical proof, many researchers have shown that the IRC guarantees variable-selection consistency for lasso-type and forward regression (Zhao and Yu, 2006; Yuan and Lin, 2007; Zhang, 2009). Intuitively, the IRC requires that informative variables and redundant variables cannot have too much ‘overlapping information’. Absent IRC, variable-selection estimators may mistakenly select redundant variables.

As shown in Definition 2.1, there are two versions of the IRC. Strong IRC is sufficient for variable-selection consistency in lasso and forward regression (Zhao and Yu, 2006; Zhang, 2009). Weak IRC is almost necessary for variable-selection consistency in lasso and forward regression (Zhao and Yu, 2006). If there exists a variable such that $\mu(F) > 1$ (e.g., \mathbf{x}_3 in Example 2), it cannot be distinguished from the informative variables due to the high level of multicollinearity. Hence, IRC is violated and variable-selection consistency cannot be

established for either lasso or forward regression (Zhao and Yu, 2006; Yuan and Lin, 2007; Zhang, 2009). Since the average L_0 solution path of solar is computed via forward regression across different subsamples, solar will also forfeit variable-selection consistency. Therefore, in this simulation, we focus on $\mu(F) \leq 1$.

We modify the DGP slightly in simulation 3 in order to control the value of $\mu(F)$. To increase the challenge of purging \mathbf{x}_5 , we choose $n = 200, p = 50$ and generate $[\mathbf{x}_0 \dots \mathbf{x}_4 \mathbf{x}_6 \dots \mathbf{x}_{50}]$ from zero-mean, unit-variance multivariate Gaussian distributions where all the correlation coefficients are 0.5.⁸ The modified DGP is as follows

$$\begin{cases} \mathbf{x}_5 = \omega \mathbf{x}_0 + \omega \mathbf{x}_1 + \gamma \cdot \sqrt{1 - 2\omega^2} \\ Y = 2\mathbf{x}_0 + 3\mathbf{x}_1 + 4\mathbf{x}_2 + 5\mathbf{x}_3 + 6\mathbf{x}_4 + e \end{cases} \quad (4.1)$$

where $\omega \in \mathbb{R}$ and γ, e are both standard Gaussian noise terms, independent from each other and all the other variables in the simulation. By setting ω to either 1/4, 1/3 or 1/2, the population value of $\mu(F)$ changes, respectively, to either 1/2, 2/3 or 1.

Figure 18 displays the directed acyclic graph of the DGP in (4.1). The variables in the DGP naturally constitute the Markov blanket of Y where \mathbf{x}_5 , the variable constructed to control $\mu(F)$, is the sibling of Y . The goal here is to recover all the informative variables for Y and to remove all the other (redundant) variables, especially \mathbf{x}_5 . Consistent with the discussion in section 2.1, we find that CV-lars-lasso and CV-cd are more likely than solar to select \mathbf{x}_5 when either weak IRC or strong IRC is satisfied.

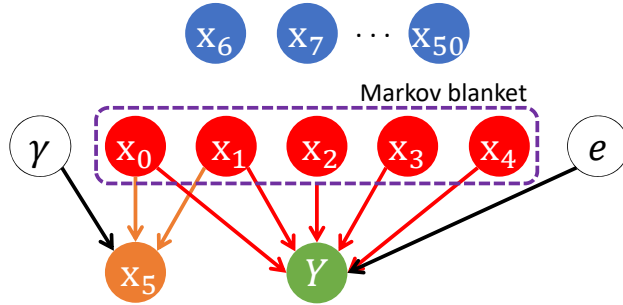


Fig 18: Directed acyclic graph of the DGP in simulation 3 with latent γ and e .

Sparsity and stability comparison

Figure 19 shows the number of variables selected in simulation 3. Since we set n and p while holding fixed the seed of the random number generator in numpy, the data for $[\mathbf{x}_0, \dots, \mathbf{x}_4, \mathbf{x}_6, \dots, \mathbf{x}_{50}]$ are identical in all 3 subplots; only the data for \mathbf{x}_5 change as ω changes. In terms of sparsity, solar outperforms CV-lars-lasso and CV-cd in all 3 subplots of Figure 19, consistent with previous results.

⁸By contrast, Zhao and Yu (2006) set the bar somewhat lower in choosing $n = 1,000$ and $p = 3$ with no correlation among the covariates.

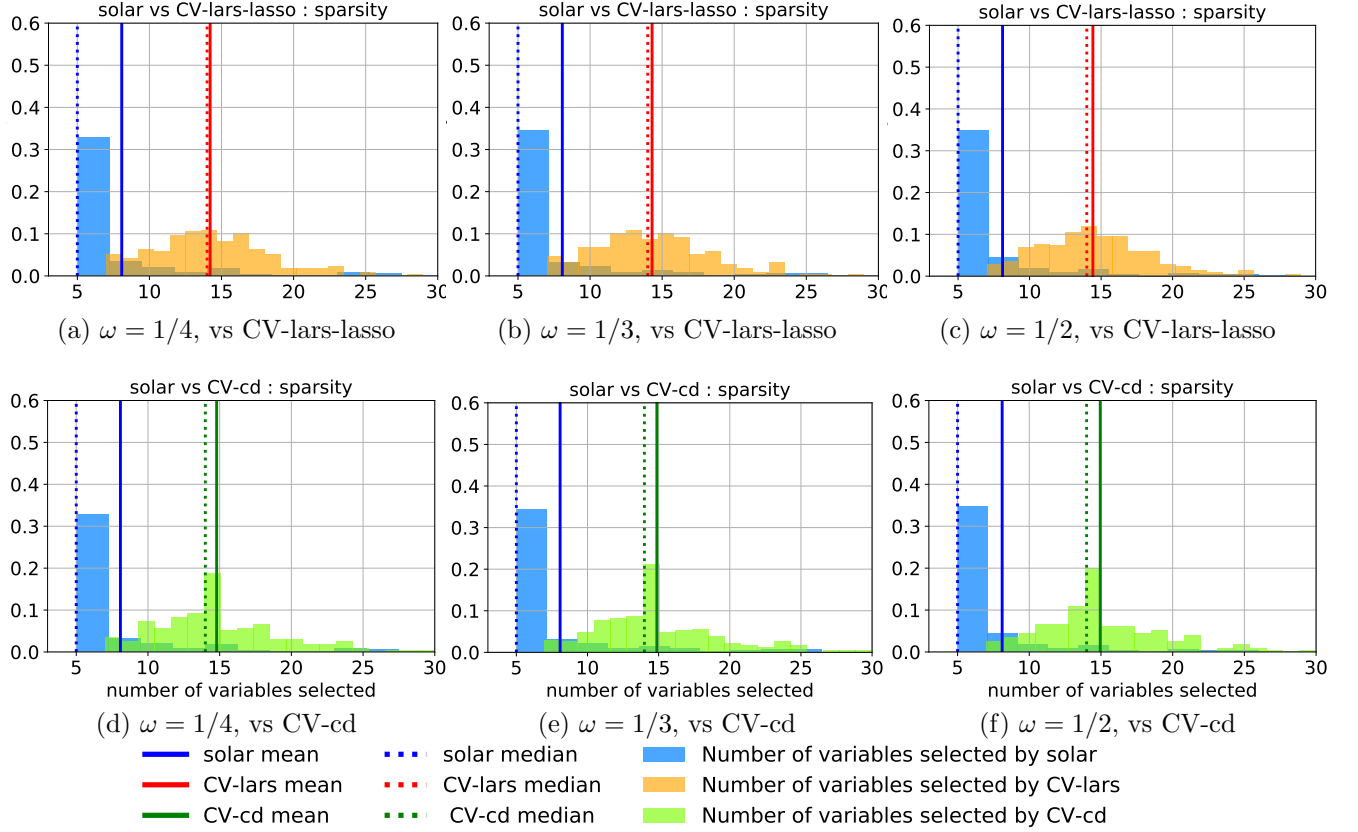


Fig 19: Histogram of the number of variables selected in simulation 3: solar vs competitors.

Because \mathbf{x}_5 is generated by a linear combination of \mathbf{x}_0 and \mathbf{x}_1 in (4.1), \mathbf{x}_5 implicitly tests the performance of solar, CV-lars-lasso and CV-cd under different settings of the IRC. In Figures 20a, 20d and 20g, $\omega = 1/4$ implies $\mu(F) = 1/2 < 1$ in the population, meaning that IRC is not violated. In Figure 20d, the probability of VSE-I(\mathbf{x}_5) for CV-cd is around 0.3, the highest probability of VSE-I error for CV-lars-lasso. Since equiangular search is more tolerant of multicollinearity than coordinate descent, the probability of VSE-I(\mathbf{x}_5) in CV-lars-lasso is slightly lower than CV-cd (Figure 20a). By contrast, owing to the extra stability due to the average L_0 solution path, the Figure 20g probability of VSE-I(\mathbf{x}_5) in solar is below 0.1. In fact, VSE-I(\mathbf{x}_5) fails to crack the top-15 list of redundant variables selected by solar when $\omega = 1/4$ (it is ranked around 50).

Comparison of variable-selection accuracy

In Figures 20b, 20e and 20h, $\omega = 1/3$, which implies $\mu(F) = 2/3$ in the population. Compared with Figure 20d, the probability of VSE-I(\mathbf{x}_5) in CV-cd clearly increases to almost 0.4, standing out from the other 9 variables. The probability of VSE-I(\mathbf{x}_5) in CV-lars-lasso is slightly lower than in CV-cd. By contrast, \mathbf{x}_5 still does not crack the top-10 list of VSE-I errors for solar (its probability remains below 0.1). When $\omega = 1/2$ in Figure 20c, 20f and 20i, $\mu(F) = 1$ in the population and strong IRC is violated, the probability of VSE-I(\mathbf{x}_5) rises to

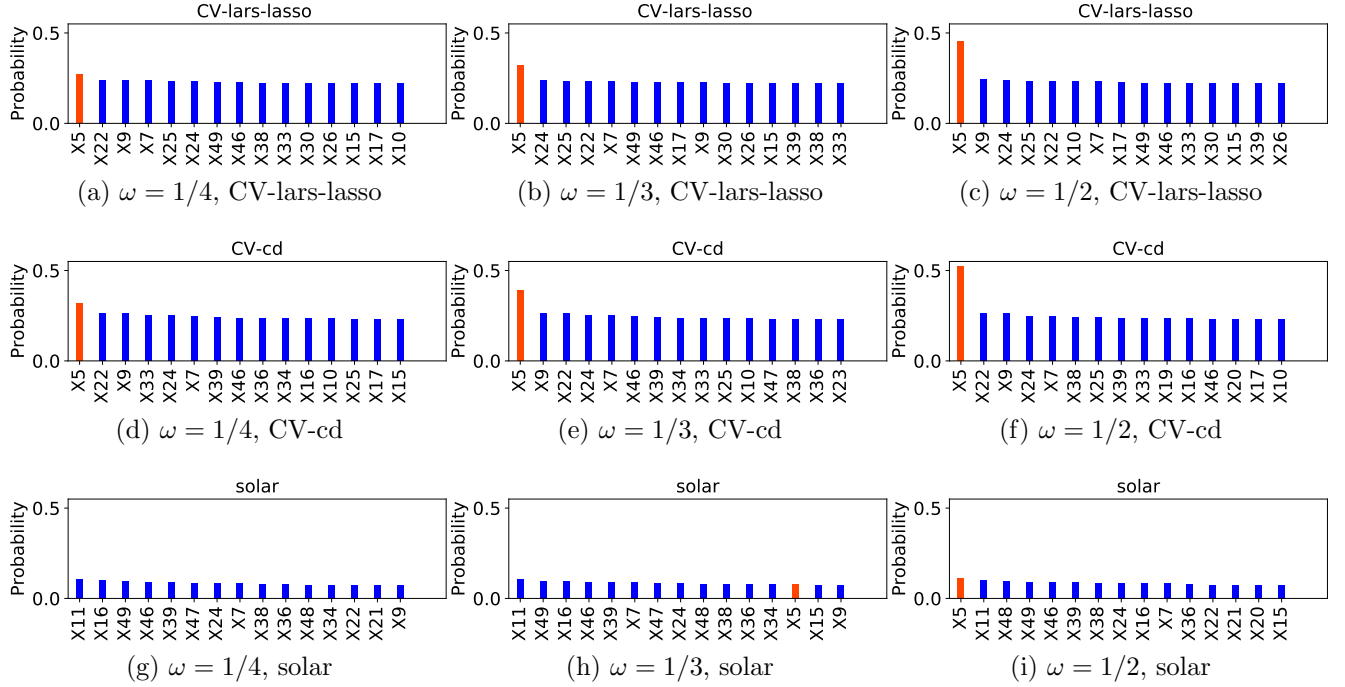


Fig 20: Probability of selecting redundant variables in simulation 3 (\mathbf{x}_5 in orange; top 15 by probability).

more than 0.4 in CV-lars-lasso and 0.5 in CV-cd. While \mathbf{x}_5 also has the highest probability of a VSE-I in solar for this case, it is only around 0.1.

The results in simulation 3 are consistent with expectation: the average L_0 solution path stabilizes the variable selection procedure. While solar, CV-lars-lasso and CV-cd all require the IRC for accurate variable selection, simulation 3 illustrates that solar is less sensitive to increases in $\mu(F)$. It is also worth noting, as Zhang (2009) suggests, that the backward-elimination option in Algorithm 3 should be used for variable selection in forward regression when $\mu(F) = 1$. Since our focus is on the solar, CV-lars-lasso and CV-cd comparison and since backward elimination may give solar an unfair edge under harsh IRC settings, we do not investigate backward elimination in the simulations.

Figure 21 shows that solar, CV-lars-lasso and CV-cd select all the informative variables with probability 1. The results are as expected given that $n = 200$ while p falls to 50.

Solar regression coefficient boxplots

The most interesting findings from simulation 3 are in Figures 20 and 22. Figure 22 reinforces the findings in Figure 20. In Figure 22a, $\omega = 1/4$ and the solar coefficient estimate for \mathbf{x}_5 fails to crack the top-15 list. A similar result obtains when ω increases to $1/3$. When ω increases to $1/2$, the solar coefficient estimate for \mathbf{x}_5 increases to 9th. However, the majority of the coefficient estimates for \mathbf{x}_5 are 0 in all 3 cases (the inter-quartile ranges, minima and maxima are all 0), illustrating the stability and sparsity of the solar coefficient estimates when $\mu(F) \leq 1$.

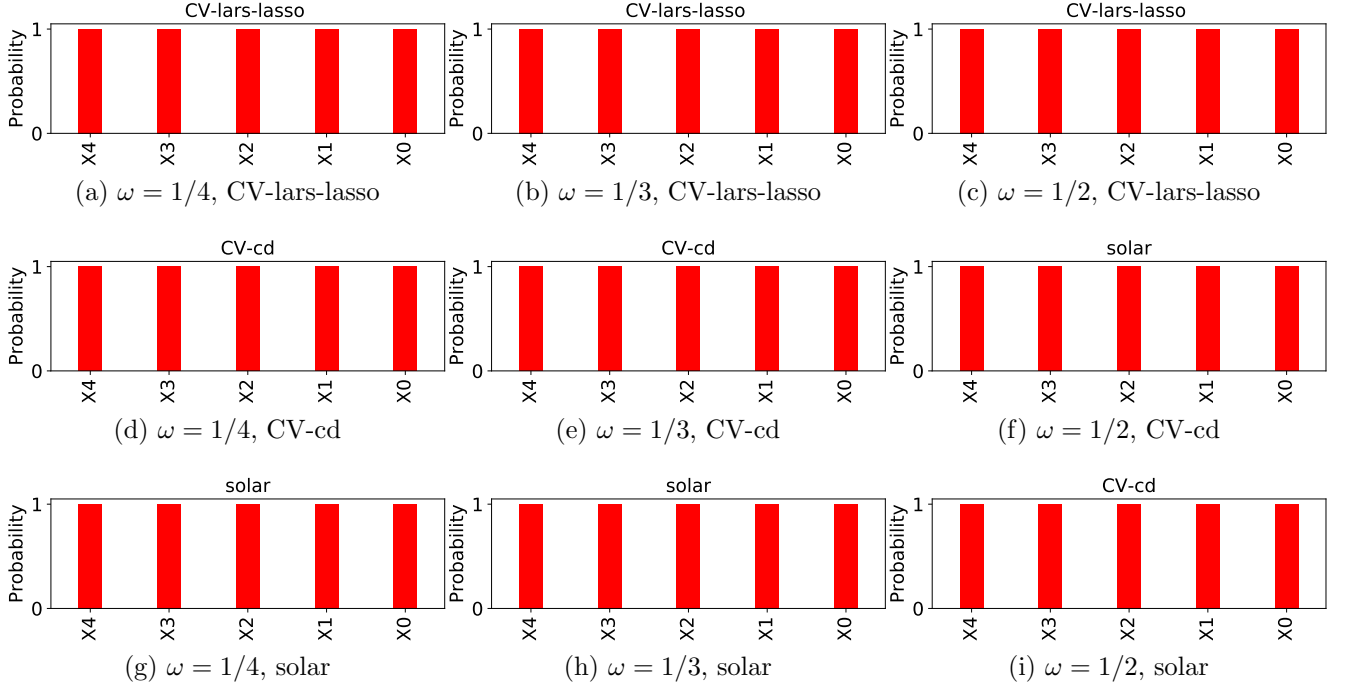


Fig 21: Probability of selecting informative variables in simulation 3.

5. Conclusion

In this paper we offer a new least-angle regression algorithm for high-dimensional data called subsample-ordered least-angle regression. We discuss the algorithm design and its computation load. We show that solar yields substantial improvements over CV-cd and CV-lars-lasso in terms of the sparsity, stability, accuracy, and robustness of variable selection. Using directed acyclic graphs, we illustrate the advantages of solar over variable screening and post-lasso selection rules for non-standard dependence structures in regression analysis.

Solar is not without its limits. A key requirement of solar is that the model must be additive; generalization to non-additive models is not guaranteed. Also, while it is an improvement on forward methods, solar still relies on the IRC to guarantee variable-selection consistency; backwards elimination may occasionally be required for high-dimensional data that violate the IRC or contain very strong noise. For cases with p over one million (typical in text mining or natural language processing), GPU parallel computation over CUDA or OpenCV is highly recommended.

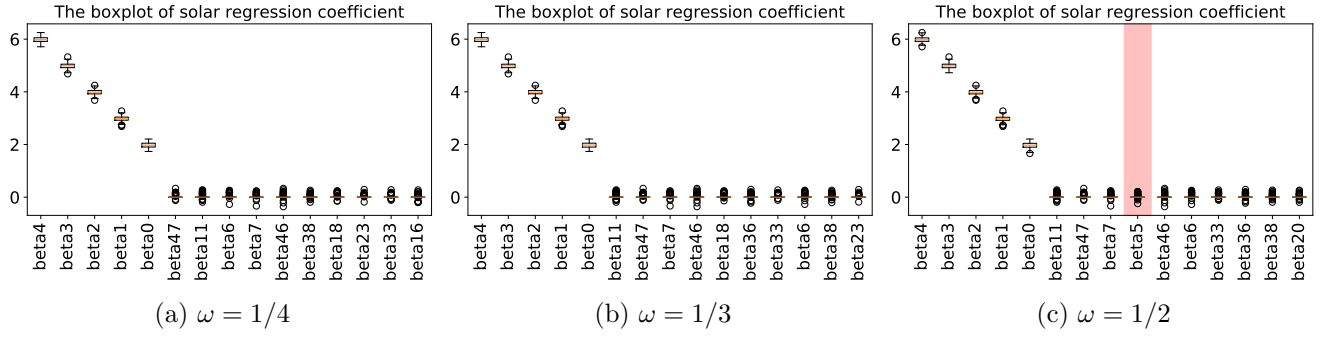


Fig 22: Solar regression coefficient boxplots in simulation 3 (top 15 by mean; β_5 in red).

Supplementary material

Read_me_first.pdf: Read this file before the other supplementary files.

Supplementary_file_A.pdf: Discussion of the latent informative variable issue in regression dependence structures.

Supplementary_file_B-Python_package.zip: Python solar package and plotting scripts for the simulation results in sections 3 and 4.

Supplementary_file_C-raw_simulation_results.zip: Complete simulation results.

References

- Bach, F.R., 2008. Bolasso: model consistent lasso estimation through the bootstrap, in: Proceedings of the 25th international conference on Machine learning, ACM. pp. 33–40.
- Bickel, P.J., Ritov, Y., Tsybakov, A.B., 2009. Simultaneous analysis of lasso and Dantzig selector. *Annals of Statistics* 37, 1705–1732.
- Candes, E.J., Plan, Y., et al., 2009. Near-ideal model selection by l1 minimization. *The Annals of Statistics* 37, 2145–2177.
- Cawley, G.C., Talbot, N.L., 2010. On over-fitting in model selection and subsequent selection bias in performance evaluation. *Journal of Machine Learning Research* 11, 2079–2107.
- Cho, H., Fryzlewicz, P., 2012. High dimensional variable selection via tilting. *Journal of the Royal Statistical Society: series B (statistical methodology)* 74, 593–622.
- Efron, B., Hastie, T., Johnstone, I., Tibshirani, R., 2004. Least angle regression. *Annals of Statistics* 32, 407–499.
- Fan, J., Lv, J., 2008. Sure independence screening for ultrahigh dimensional feature space. *Journal of the Royal Statistical Society: Series B (Statistical Methodology)* 70, 849–911.
- Friedman, J., Hastie, T., Tibshirani, R., 2001. The elements of statistical learning. volume 1 of *Springer Series in Statistics*. Springer-Verlag New York.
- Friedman, J., Hastie, T., Tibshirani, R., 2008. Sparse inverse covariance estimation with the graphical lasso. *Biostatistics* 9, 432–441.
- Friedman, J., Hastie, T., Tibshirani, R., 2010. A note on the group lasso and a sparse group lasso. arXiv e-print 1001.0736 .
- Friedman, J., Hastie, T., Tibshirani, R., 2010. Regularization paths for generalized linear models via coordinate descent. *Journal of statistical software* 33, 1.

- Ghaoui, L.E., Viallon, V., Rabbani, T., 2010. Safe feature elimination for the lasso and sparse supervised learning problems. arXiv preprint arXiv:1009.4219 .
- Hall, P., Miller, H., 2009. Using generalized correlation to effect variable selection in very high dimensional problems. *Journal of Computational and Graphical Statistics* 18, 533–550.
- Hall, P., Miller, H., et al., 2009. Using the bootstrap to quantify the authority of an empirical ranking. *The Annals of Statistics* 37, 3929–3959.
- Hastie, T., Efron, B., 2013. Least Angle Regression, Lasso and Forward Stagewise. R Foundation for Statistical Computing. URL: <https://cran.r-project.org/web/packages/lars>. r package version 1.2.
- Jia, J., Yu, B., 2010. On model selection consistency of the elastic net when $p \gg n$. *Statistica Sinica* , 595–611.
- Knight, K., Fu, W., 2000. Asymptotics for lasso-type estimators. *Annals of Statistics* 28, 1356–1378.
- Koller, D., Friedman, N., 2009. Probabilistic graphical models: principles and techniques. MIT press.
- Li, G., Peng, H., Zhang, J., Zhu, L., et al., 2012a. Robust rank correlation based screening. *The Annals of Statistics* 40, 1846–1877.
- Li, R., Zhong, W., Zhu, L., 2012b. Feature screening via distance correlation learning. *Journal of the American Statistical Association* 107, 1129–1139.
- Lim, C., Yu, B., 2016. Estimation stability with cross-validation (ESCV). *Journal of Computational and Graphical Statistics* 25, 464–492.
- Lockhart, R., Taylor, J., Tibshirani, R.J., Tibshirani, R., 2014. A significance test for the lasso. *Annals of statistics* 42, 413.
- Meinshausen, N., 2007. Relaxed lasso. *Computational Statistics & Data Analysis* 52, 374–393.
- Meinshausen, N., Bühlmann, P., 2010. Stability selection. *Journal of the Royal Statistical Society: Series B (Statistical Methodology)* 72, 417–473.
- Meinshausen, N., Yu, B., 2009. Lasso-type recovery of sparse representations for high-dimensional data. *Annals of Statistics* 37, 246–270.
- Nan, Y., Yang, Y., 2014. Variable selection diagnostics measures for high-dimensional regression. *Journal of Computational and Graphical Statistics* 23, 636–656.
- Pedregosa, F., Varoquaux, G., Gramfort, A., Michel, V., Thirion, B., Grisel, O., Blondel, M., Prettenhofer, P., Weiss, R., Dubourg, V., Vanderplas, J., Passos, A., Cournapeau, D., Brucher, M., Perrot, M., Duchesnay, E., 2011. Scikit-learn: Machine learning in Python. *Journal of Machine Learning Research* 12, 2825–2830.
- Shao, X., Zhang, J., 2014. Martingale difference correlation and its use in high-dimensional variable screening. *Journal of the American Statistical Association* 109, 1302–1318.
- Stone, M., 1974. Cross-validatory choice and assessment of statistical predictions. *Journal of the Royal Statistical Society, Series B (Methodological)* 36, 111–147.
- Stone, M., 1977. An asymptotic equivalence of choice of model by cross-validation and Akaike’s criterion. *Journal of the Royal Statistical Society, Series B (Methodological)* 39, 44–47.
- Tibshirani, R., 1996. Regression shrinkage and selection via the Lasso. *Journal of the Royal Statistical Society, Series B (Methodological)* 58, 267–288.
- Tibshirani, R., Bien, J., Friedman, J., Hastie, T., Simon, N., Taylor, J., Tibshirani, R.J.,

2012. Strong rules for discarding predictors in lasso-type problems. *Journal of the Royal Statistical Society: Series B (Statistical Methodology)* 74, 245–266.
- Tibshirani, R., Saunders, M., Rosset, S., Zhu, J., Knight, K., 2005. Sparsity and smoothness via the fused lasso. *Journal of the Royal Statistical Society: Series B (Statistical Methodology)* 67, 91–108.
- Tropp, J.A., 2004. Greed is good: Algorithmic results for sparse approximation. *IEEE Transactions on Information theory* 50, 2231–2242.
- Wainwright, M.J., 2009. Sharp thresholds for high-dimensional and noisy sparsity recovery using ℓ_1 -constrained quadratic programming (lasso). *IEEE transactions on information theory* 55, 2183–2202.
- Wang, J., Zhou, J., Liu, J., Wonka, P., Ye, J., 2014. A safe screening rule for sparse logistic regression, in: *Advances in neural information processing systems*, pp. 1053–1061.
- Wang, Y., Chen, X., Ramadge, P.J., 2016. Feedback-controlled sequential lasso screening. *arXiv preprint arXiv:1608.06010*.
- Weisberg, S., 2004. Discussion following “Least angle regression,” by B. Efron, T. Hastie, I. Johnstone, and R. Tibshirani. *Annals of Statistics* 32, 490–494.
- Wu, T.T., Lange, K., et al., 2008. Coordinate descent algorithms for lasso penalized regression. *The Annals of Applied Statistics* 2, 224–244.
- Xu, G., Huang, J.Z., et al., 2012. Asymptotic optimality and efficient computation of the leave-subject-out cross-validation. *The Annals of Statistics* 40, 3003–3030.
- Yuan, M., Lin, Y., 2007. On the non-negative garrotte estimator. *Journal of the Royal Statistical Society: Series B (Statistical Methodology)* 69, 143–161.
- Zeng, Y., Yang, T., Breheny, P., 2017. Efficient feature screening for lasso-type problems via hybrid safe-strong rules. *arXiv preprint arXiv:1704.08742*.
- Zhang, T., 2009. On the consistency of feature selection using greedy least squares regression. *Journal of Machine Learning Research* 10, 555–568.
- Zhao, P., Yu, B., 2006. On model selection consistency of Lasso. *Journal of Machine Learning Research* 7, 2541–2563.
- Zou, H., 2006. The adaptive lasso and its oracle properties. *Journal of the American statistical association* 101, 1418–1429.
- Zou, H., Hastie, T., 2005. Regularization and variable selection via the elastic net. *Journal of the royal statistical society: series B (statistical methodology)* 67, 301–320.